Studies on Toxicity Assessment of Industrial Materials

Studies on Toxicity Assessment of Industrial Materials

(産業材料の毒性評価に関する研究)

2019

The United Graduate School of Agricultural Science, Gifu University

Science of Biological Resources

(Gifu University)

MORIYAMA, Akihiro

Studies on Toxicity Assessment of Industrial Materials

(産業材料の毒性評価に関する研究)

MORIYAMA, Akihiro

CONTENTS

1. OVERVIEW

The development of industrial products using nanomaterials and their application to the medical and environmental fields are energetically advanced on a global scale, but at the same time there are concerns about the effect on humans and the environment. The purpose of this study was to investigate the toxicity and biological effects of industrial materials such as nanoparticles and carbon fiber by using molecular biological techniques.

2. EXPERIMENTS

2-1 *The effects of titanium dioxide nanoparticles and UV irradiation on yeast cells*

2-1-1 INTRODUCTION

A nanoparticle is defined as a nano-object with all ext\ernal dimensions in the nanoscale (length range approximately from 1 nm to 100 nm), where the lengths of the longest and the shortest axes of the nano-object do not differ significantly[1]. Compared with a fine particle, the nanoparticle has a larger specific surface area. Therefore, nanoparticles show greater chemical and physical activities, such as ion release, adsorption ability, and production of reactive oxygen species (ROS)[2]. The unique properties of nanoparticles are beneficial, and thus, the use of nanoparticles is expanding rapidly.

TiO_2 nanoparticles are used in various commercial products (e.g., self-cleaning surface coatings, light-emitting diodes, solar cells, disinfectant sprays, sporting goods, drinking water treatment agents, and topical sunscreens) because of their catalytic activity and UV absorption (λ<400 nm)[3]. They are not dissolved in water, and generate ROS under UV irradiation, apparently enabling them to decompose organic substances and damage the function and structure of various cells[4].The catalytic activity of TiO_2 nanoparticles was believed to be capable of killing a wide range of microorganisms (e.g. gram-negative and gram-positive bacteria, including endospores, as well as fungi, algae, protozoa, and viruses)[5].

In culture medium and the water environment, nanoparticles unexceptionally form structures of their aggregates and agglomerates comprising primary particles. These

compounds are defined as NOAAs (nano-objects, and their aggregates and agglomerates greater than 100 nm)[6]. An aggregate is a particle that comprises strongly bonded or fused single primary particles, and an agglomerate is a collection of weakly bound single primary particles, aggregates, or a mix of these. The name NOAA is made by International Standard Organization[1] to share the knowledge that nanoparticles may not be protected for aggregation and agglomeration and can not be alone as single molecule in culture medium and water environment. The unique properties of TiO_2 nanoparticles can be maintained in the environment, and thus the increasing use of TiO_2 nanoparticles is raising environmental concerns. An assessment of the biological and ecological effects of TiO_2-NOAAs is necessary.

In our previous study, we assessed the effect of TiO_2-NOAAs on microbes using *Saccharomyces cerevisiae* and *Escherichia coli*. The TiO_2-NOAAs decomposed methylene blue under UV irradiation, which suggested that the TiO_2-NOAAs generated ROS under UV irradiation. However, the TiO_2-NOAAs did not demonstrate growth inhibition in minimal agar medium under UV irradiation; the addition of TiO_2-NOAAs to the medium still permitted colony formation under a UV intensity that inactivates microbes. Moreover, the TiO_2-NOAAs adsorbed microbes. These results suggested that the amount of ROS generated by TiO_2-NOAAs was insufficient to inactivate microbes, and the TiO_2-NOAAs might protect microbes from UV[7].

In this study, we assessed the effect of TiO_2-NOAAs under UV on *S. cerevisiae* in more detail. We used DNA microarray analysis for qualitative assessment of gene expression profile and carried out a quantitative assessment using qRT-PCR method. These results suggest the effect of TiO_2-NOAAs on yeast cells under UV irradiation is not caused by TiO_2-NOAA but UV irradiation.

2-1-2 MATERIALS AND METHODS

2-1-2-1 Materials

TiO_2 nanoparticles were obtained from Ishihara Sangyo Kaisha, Ltd. (Japan). Their crystals were in the anatase form, with a primary particle size of 7 nm, and a specific surface area of 316 m^2/g.

2-1-2-2 Yeast strains and growth conditions

S. cerevisiae S288C (*MATα SUC2 mal mel gal2 CUP1* [cir^+]) was used in this

study. The yeast was grown in minimal medium (0.67% Difco™ Yeast Nitrogen Base w/o Amino Acids (Becton, Dickinson and Company, NJ, USA), 2% D(+)-Glucose) at 30 °C. A pre-culture was incubated to stationary phase (2 days).

2-1-2-3 TiO_2 nanoparticle treatment

One mL of pre-culture (5×10^7 cells) and 19 mL of minimal medium were added to petri dishes (φ 90 mm × 20 mm). They were incubated for 6 h at 30 °C with shaking at 60 rpm to produce exponentially growing cells. Then, 5.0 mg of TiO_2 nanoparticles were added to the petri dishes, with or without UV irradiation (intensity; 0.01 mW/cm^2), and the cells were incubated for a further 2h. Treated yeast cells were divided into the adsorbed fraction and non-adsorbed fractions. Each of the yeast under different conditions (Condition 1. adsorbed fraction to TiO_2-NOAA under UV irradiation, 2. non-adsorbed fraction to TiO_2-NOAA under UV irradiation, 3. adsorbed fraction to TiO_2-NOAA without UV irradiation, 4. non-adsorbed fraction to TiO_2-NOAA without UV irradiation, 5. under UV and 6. untreated control) was harvested by centrifugation at 2150×*g* for 3 min at 4 °C (CAX-371; Tomy Seiko Co., LTD., Tokyo, Japan). Under our TiO_2 nanoparticles treatment conditions (30 °C with shaking at 60 rpm), many yeasts aggregated with NOAAs. However, we could yield enough yeast cells for DNA microarray in the supernatant phase over the NOAA and yeast agglomerates (Condition 2, 4).

2-1-2-4 RNA extraction

RNA was extracted from cells using a Fast RNA® Pro Red Kit (MP Biomedicals, Santa Ana, CA, USA), according to the manufacturer's instructions, with the following exceptions: cell disruption was performed for 10 min using a Multi-Beads Shocker®(Yasui Kikai, Osaka, Japan) and chloroform (Wako Pure Chemical Industries) treatment was performed twice. The extracted RNA was purified using a Qiagen RNeasy Mini kit (Qiagen GmbH, Hilden, Germany), according to the manufacturer's instructions. The quality of the purified RNA was verified using an Agilent® 2100 Bioanalyzer (Agilent Technologies, CA, USA). The RNA concentration was determined using a Micro-volume Spectrophotometer Q5000 (Tomy Seiko Co., LTD).

2-1-2-5 DNA microarray analysis

DNA microarray analysis was carried out to assess the effect of TiO_2-NOAAs on yeast qualitatively.

Fluorescent cyanine 3-cytidine triphosphate (CTP)-labeled cRNA was synthesized using a Quick Amp Labeling Kit (Agilent Technologies, CA, USA). The CTP-labeled cRNA was used for hybridization to Yeast (V2) Gene Expression Microarray slides (#G4813A016322, Agilent Technologies) at 65 °C for 17 h. The hybridized microarray slides were washed according to the manufacturer's instructions and scanned using an Agilent DNA Microarray Scanner (#G2565CA, Agilent Technologies) at a resolution of 5 μm. The scanned images were analyzed quantitatively using the Agilent Feature Extraction Software version 10.7.3.1 (Agilent Technologies).

Signals detected from each open reading frame (ORF) were normalized using the 25th percentile and quantile methods. The genes classified as upregulated or downregulated were those that passed the Student's *t*-test ($P< 0.05$) and exhibited more than 2-fold higher intensities or more than 0.5-fold lower intensities than that of negative control.

The gene expression profiles were characterized according to the categories of the Munich Information Center for Protein Sequences Genome Research Environment Comprehensive Yeast Genome Database (MIPS GenRE CYGD, http://mips.helmholtz-muenchen.de/genre/proj/yeast/index.jsp) and the *Saccharomyces* Genome Database (SGD, http://www.yeastgenome.org/).The DNA microarray experiments described in this study were MIAME compliant and the raw data has been deposited in the Gene Expression Omnibus (GEO) database under the accession number GSE99660. For each condition, RNA samples were prepared at least four replications.

2-1-2-6 Quantitative PCR

qRT-PCR was carried out to assess the effect of TiO_2-NOAAs on yeast cells quantitatively.

The RNA used for DNA microarray analysis was subjected to reverse transcription (RT) at 37 °C for 15 min using a ReverTra Ace® qPCR RT Master Mix (Toyobo, Osaka, Japan). For quantitative PCR amplification, the Power SYBR® Green Master Mix (Applied Biosystems, CA, USA) and StepOnePlus™ real-time PCR System (Applied Biosystems) were used, as described in the manufacturer's instructions (holding at 95 °C

for 10 min, followed by 40 cycles of denaturation at 95 °C for 15 sec, and annealing and extension at 60 °C for 2 min). Relative expression levels were calculated from Ct values. Five pairs of primers were designed for the amplification of the genes upregulated under certain conditions (Table 1), based on the results of DNA microarray analysis. All experiments were performed in triplicate.

Table 1. Sequences of oligonucleotide primers used in this study

Gene name	**F-primer**	**R-primer**
GRE2	AAGGTCATCGGTTCTGCCAG	CCTTGCCGTGCTTTTGGAAA
SOD2	CTCCCGCAAACGCAAGAAAA	CTCGTCCAGACTGCCAAACT
GSY1	CATATGGGCCATCGTCGTCA	GGTACCTAAATCGCCCGGAG
TPS2	CGCAGCTGCCCTACAAAATC	TGGGTCATCGTCCAGATCCT
ACT1	ATTGCCGAAAGAATGCAAAAGG	CGCACAAAAGCAGAGATTAGAAACA

The *ACT1* gene was used as a control housekeeping gene because little difference in its gene expression level was observed between the treatment groups and a control from the result of DNA microarray analysis, and it is widely accepted as a positive control to study the yeast stress response[8].

2-1-3 RESULTS AND DISCUSSION

2-1-3-1 Conditions for TiO_2 nanoparticle treatment

To assess the effect of TiO_2-NOAAs on yeast cells at the RNA level, initially, an appropriate intensity of UV irradiation was determined (Fig. 1).

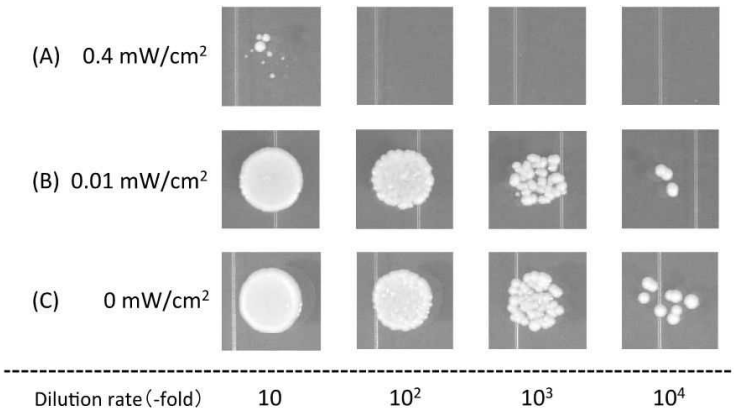

Fig. 1. Viable yeast cell numbers under each UV irradiation intensity. Yeast cells were incubated under the same conditions with TiO_2 nanoparticle treatment (as described in the text) under various UV irradiation intensities. To determine their viabilities, yeast cells were serially diluted and incubated on minimal agar media for 2–3 days.

Under the strongest UV intensity, 0.4 mW/cm^2 (A), few yeast cells survived, thus their RNA could not be extracted. Under a UV intensity of 0.01 mW/cm^2 (B), UV inactivation of the yeast cells was observed, and their RNA could be extracted. Therefore, RNA extraction for the DNA microarray and qRT-PCR was conducted at a UV intensity of 0.01 mW/cm^2.

The treatment concentration of TiO_2 nanoparticle was the same as that used in our previous study[7]. It is also confirmed that when titanium is added to the minimum medium, it aggregates to form NOAA. Furthermore, it was also confirmed that many yeasts are adsorbed to TiO_2 nanoparticles when co-culturing yeast cells (Fig. 2).

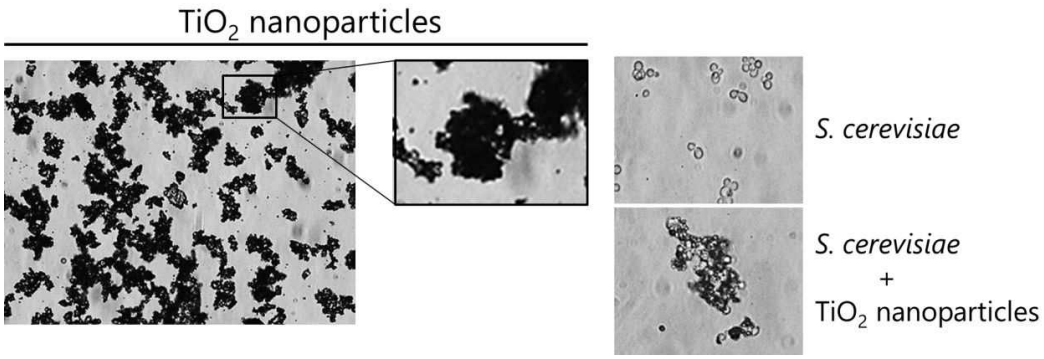

Fig. 2. A state of agglomerates of TiO_2 nanoparticles and yeast. 1 mL of pre-culture (5×10^7 cells), 19 mL of minimal medium and 5.0 mg of TiO_2 nanoparticles were added to the petri dishes (φ 90 mm × 20 mm).

2-1-3-2 Qualitative assessment of the effect of TiO_2-NOAA on yeast by DNA microarray analysis

2-1-3-2-1 Overview of altered genes in each treatment condition

In this study, yeast cells from six different treatment conditions (1. adsorbed fraction to TiO_2-NOAA under UV irradiation, 2. non-adsorbed fraction to TiO_2-NOAA under UV irradiation, 3. adsorbed fraction to TiO_2-NOAA without UV irradiation, 4. non-adsorbed fraction to TiO_2-NOAA without UV irradiation, 5. under UV and 6. untreated control) were analyzed using a DNA microarray. From the results, 3236, 1545, 2914, 1596, and 2493 ORFs that passed the Student's *t*-test ($P < 0.05$) in Conditions 1, 2, 3, 4, and 5, respectively, were obtained by the comparison with untreated control of 6 (Table 2).

Table 2. The number of the up and downregulated genes in each treatment condition

Treatment conditions	**≧2-fold**	**≦0.5-fold**
1. Adsorbed fraction of TiO_2-NOAA (with UV)	275	425
2. Non-adsorbed fraction of TiO_2-NOAA (with UV)	9	109
3. Adsorbed fraction of TiO_2-NOAA (without UV)	219	287
4. Non-adsorbed fraction of TiO_2-NOAA (without UV)	18	121
5. Under UV	59	223

Among them, 275, 9, 219, 18, and 59 genes exhibited more than 2-fold higher intensities, and 425, 109, 287, 121, and 223 genes exhibited more than 0.5-fold lower intensities under Conditions 1, 2, 3, 4, and 5, respectively. The highest number of significantly altered genes was in Conditions 1 (2-fold; 275, 0.5-fold; 425), 3 (2-fold; 219, 0.5-fold; 287), and 5 (2-fold; 59, 0.5-fold; 223).

These results showed that the expressions of genes in yeast cells that were adsorbed by TiO_2-NOAAs (Conditions 1 and 3) were altered more than those in yeast cells that were not adsorbed by TiO_2-NOAAs (Conditions 2 and 4). Further, a significant number of genes were altered by UV irradiation in the adsorbed fraction (Condition 1). Thus, these results suggested that yeast cells suffer stress from TiO_2-NOAA and from UV.

2-1-3-2-2 The genes up and downregulated by TiO_2-NOAAs under UV irradiation and their functional distribution

The yeast cells in the fraction adsorbed to TiO_2-NOAA under UV irradiation showed the highest number of genes with altered expressions among all treatment conditions (Table 2; Condition 1).From the DNA microarray analysis, 3236 ORFs were obtained that passed the Student's *t*-test ($P < 0.05$). Among them, 275 genes were upregulated by more than 2-fold and 425 were downregulated by more than 0.5-fold by TiO_2-NOAA treatment under UV irradiation. The up and downregulated genes were characterized using MIPS GenRE CYGD. The results showed that the function of upregulated genes were classified with the high probability into the categories of "energy (10.3%)", "cell rescue (7.4%)" and "metabolism (6.0%)". Subcategories of "Regulation of glycolysis and gluconeogenesis" and "metabolism of energy reserve (e.g. glycogen, trehalose)" were characterized particularly in the category of "energy" (Fig. 3).

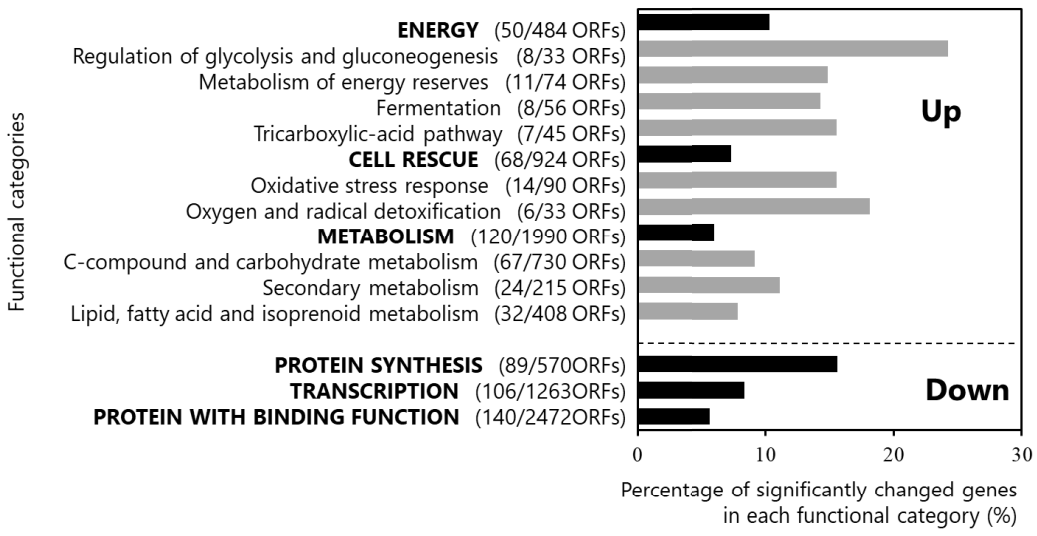

Fig. 3. Functional categories of up-regulated and down-regulated ORFs in TiO_2-NOAA treatment under UV irradiation (Condition 1). ORFs up-regulated or down-regulated more than 2 fold were counted. The denominators and numerators in parentheses indicate number of total ORFs and up-regulated or down-regulated ORFs in each category, respectively.

.

Trehalose stabilizes the membrane structure and glycogen is a component of the cell wall in *S. cerevisiae*[9, 10]. Subcategories of "oxidative stress response" and "oxygen and radical detoxification" were characterized particularly in the category of "cell rescue".

By contrast, downregulated genes were characterized particularly in the categories of "protein synthesis (16%)", "transcription (8%)", and "protein with binding function (6%)" (Fig. 3). Genes involved in protein synthesis are downregulated in response to diverse environmental stresses[11]. Thus, this result suggested that yeast cells adsorbed by TiO_2-NOAAs under UV irradiation were significantly stressed.

The products of the upregulated genes were localized significantly at the "peroxisome" (Fig. 4).

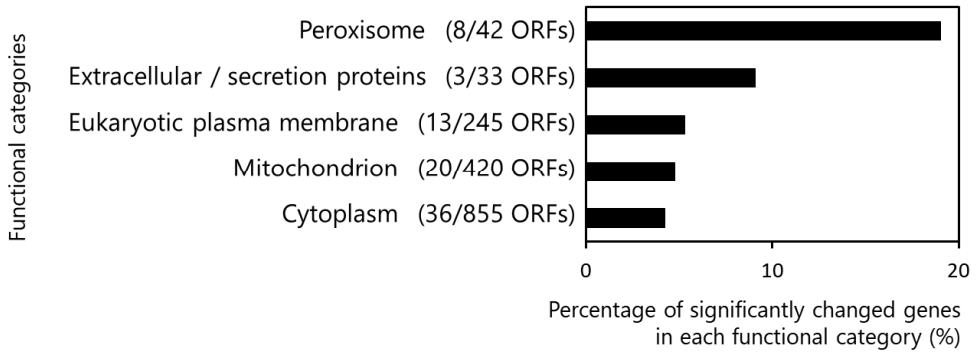

Fig. 4. Locational categories of the gene products upregulated by TiO_2-NOAA treatment under UV irradiation (Condition 1). ORFs up-regulated more than 2 fold were counted. The denominators and numerators in parentheses indicate number of total ORFs and up-regulated ORFs in each category, respectively.

It is reported that some peroxisomal genes are induced in response to oxidative stress[12]. Thus, this localization and induction of subcategories related to oxidative stress suggested that yeast cells that were adsorbed by TiO_2-NOAA under UV irradiation suffered oxidative stress. Additionally, localization with high probability at "Extracellular/secretion proteins" and "Eukaryotic plasma membrane" were observed.

2-1-3-2-3 Genes upregulated and downregulated by TiO_2-NOAAs without UV irradiation and their functional distribution

The expressions of a significant number of genes in yeast cells in the adsorbed fraction to TiO_2-NOAAs even without UV irradiation were altered in all treatment conditions (Table 2; Condition 3). From the DNA microarray analysis, 2914 ORFs were obtained that passed the Student's *t*-test ($P < 0.05$). Among them, 219 genes were upregulated by more than 2-fold and 287 genes were downregulated by more than 0.5-fold by TiO_2-NOAAs treatment without UV irradiation. The functions of the upregulated genes were classified with high probability into the categories of "energy (8.9%)", "metabolism (5.1%)", and "cell rescue (5.7%)". Subcategories of "metabolism of energy reserve (e.g. glycogen, trehalose)" and "regulation of glycolysis and gluconeogenesis" were classified particularly in the category of "energy", and subcategories of "C-compound and carbohydrate metabolism" was classified particularly in the category of "metabolism" (Fig. 5).

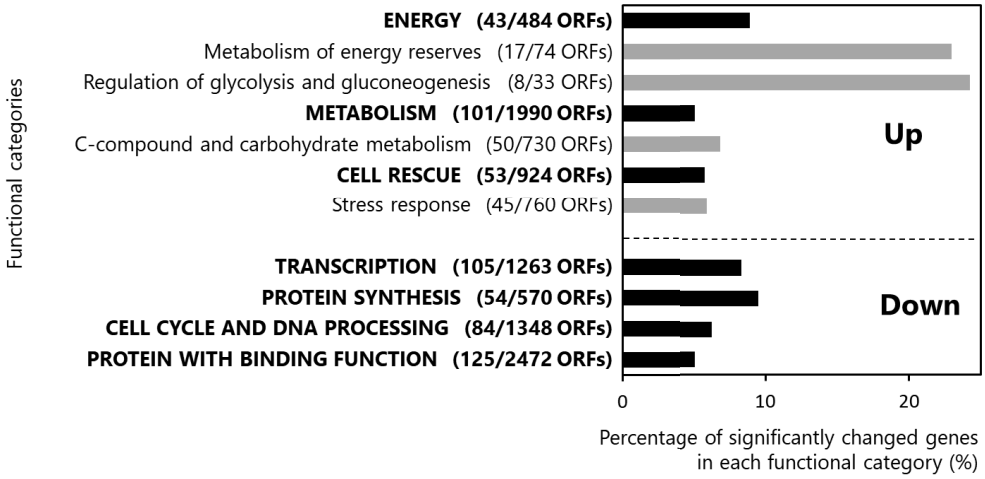

Fig. 5. Functional categories of the genes upregulated and downregulated by TiO_2-NOAA treatment without UV irradiation (Condition 3). ORFs up-regulated or down-regulated more than 2 fold were counted. The denominators and numerators in parentheses indicate number of total ORFs and up-regulated or down-regulated ORFs in each category, respectively.

By contrast, the functions of the downregulated genes were classified as "transcription (8.3%)", "protein synthesis (9.5%)", and "cell cycle and DNA processing (6.2%)" (Fig. 5). This result showed that the yeast that were adsorbed by TiO_2-NOAA without UV irradiation suffered stress. The products of the upregulated genes were localized as "Eukaryotic plasma membrane" (Fig. 6).

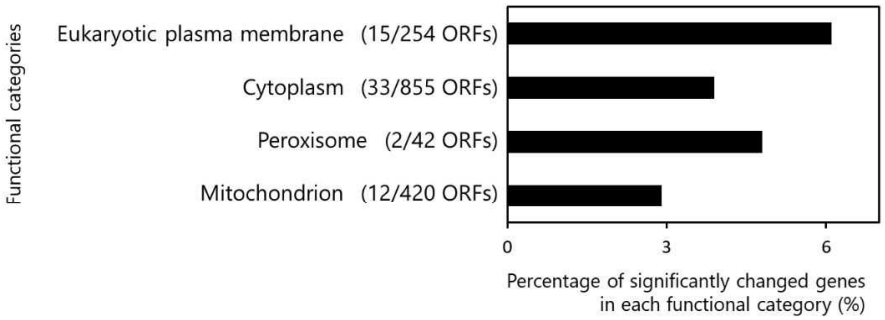

Fig. 6. Locational categories of the genes upregulated by TiO_2-NOAA treatment under UV irradiation (Condition 3). ORFs up-regulated more than 2 fold were counted. The denominators and numerators in parentheses indicate number of total ORFs and up-regulated ORFs in each category, respectively.

These results showed that membrane structures of yeast cells that were adsorbed by TiO_2-NOAA without UV irradiation were damaged. Taken together, these results imply yeast cells that are adsorbed by TiO_2-NOAA without UV irradiation suffer stress at their membrane structures, resulting in the induction of genes related to the synthesis of glycogen and trehalose.

2-1-3-2-4 Genes upregulated and downregulated by UV irradiation and their functional distribution

The expressions of a large number of genes in yeast cells under UV without TiO_2-NOAAs were altered among all treatment conditions (Table 2; Condition 5). From the DNA microarray analysis, 2493 ORFs were obtained that passed the Student's *t*-test ($P < 0.05$). Among them, 59 genes were upregulated by more than 2-fold and 223 genes were downregulated by more than 0.5-fold by UV irradiation. The functions of the upregulated genes were classified with high probability into the categories of "energy (2.5%)", "cell rescue (1.7%)", and "metabolism (3.6%)" (Fig. 7). The subcategory of "metabolism of energy reserve" was characterized particularly in the category of "energy", and subcategories of "oxygen and radical detoxification" were characterized particularly in the category of "cell rescue". This result showed that yeast cells that are irradiated by UV suffer oxidative stress. The localizations of the products of the upregulated genes were not found because of the insignificant number of genes in this category.

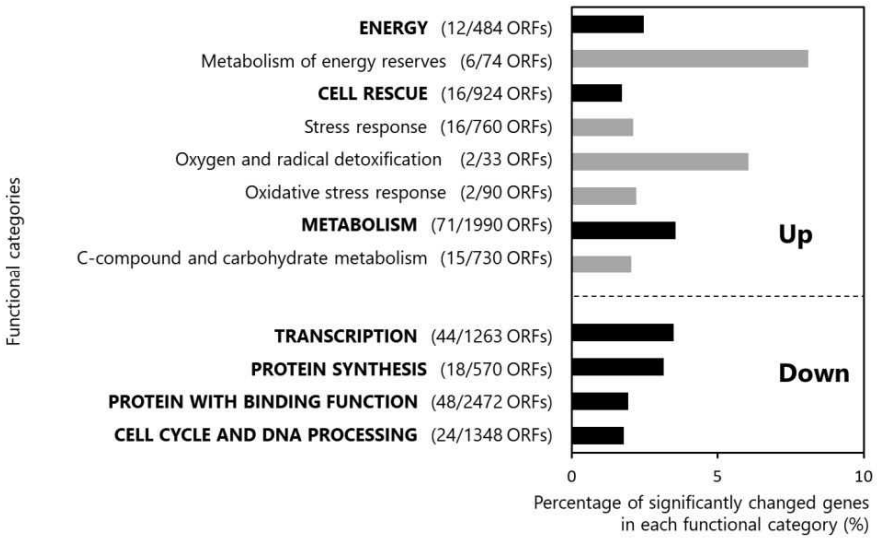

Fig. 7. Functional categories of the genes upregulated by UV irradiation (Condition 5). ORFs up-regulated or down-regulated more than 2 fold were counted. The denominators and numerators in parentheses indicate number of total ORFs and up-regulated or down-regulated ORFs in each category, respectively.

By contrast, the functions of the downregulated genes were classified with high probability into the categories of “transcription (3.5%)” and “protein synthesis (3.2%)” (Fig. 7). These results showed that yeast cells that were irradiated by UV suffered stress.

These results suggested that yeast cells irradiated by UV suffer oxidative stress because genes involved in the response to oxidative stress were upregulated, and genes involved in protein synthesis were downregulated.

2-1-3-3 Quantitative assessment of the effect of TiO_2-NOAAs on yeast by qRT-PCR

From the result of the DNA microarray analysis, the upregulated genes in this study were mainly involved in response to reserving energy sources and an oxidative stress. In particular, we found that the gene related to reserving energy is induced under condition 3, and the gene related to oxidative stress is induced under condition 1 (Fig. 8).

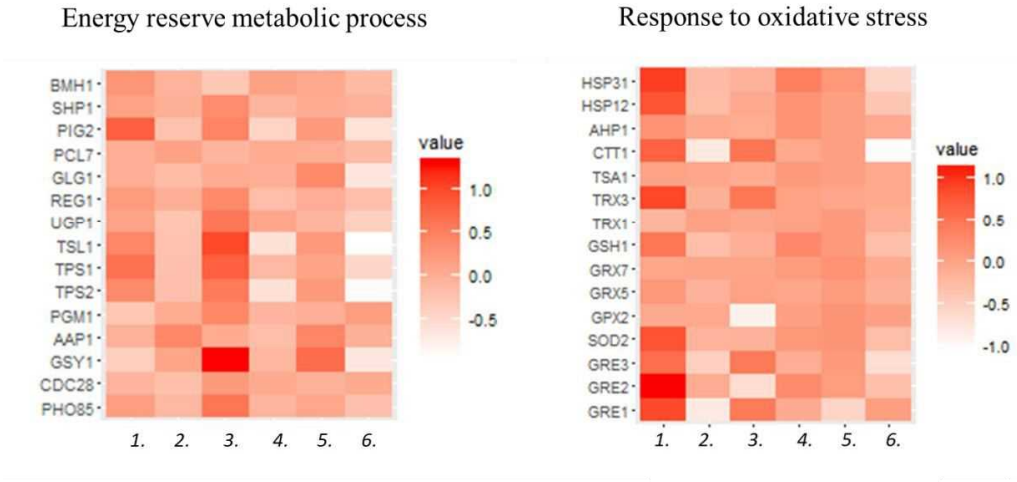

Fig. 8. Gene expression of the genes related to “response to oxidative stress” (GO:0006979, left) and “energy reserve metabolic process”(GO:0006112, right) in each conditions. Red color indicates up-regulation. 1. adsorbed fraction to TiO_2-NOAA under UV; 2. non-adsorbed fraction to TiO_2-NOAA under UV; 3. adsorbed fraction to TiO_2-NOAA without UV; 4. non-adsorbed fraction to TiO_2-NOAA without UV; 5. under UV; 6. untreated control.

Thus, we tried to assess the stress levels quantitatively using qRT-PCR. The *GRE2* and *SOD2* genes were used as indicators of the level of response to oxidative

stress, and the *GSY1* and *TPS2* genes were used as indicators of the levels of reserving energy sources.

The genes involved in oxidative stress were upregulated in UV treatment Conditions 1 (*GRE2*; 2.0-fold, *SOD2*; 1.8-fold), 2 (*GRE2*; 3.1-fold, *SOD2*; 2.4-fold), and 5 (*GRE2*; 3.8-fold, *SOD2*; 2.8-fold) (Fig. 9). This result suggested yeast cells that are exposed to UV suffer oxidative stress. In addition, oxidative stress was caused under UV not presence of TiO_2-NOAA. This shows UV stress is more dominant than that caused by TiO_2-NOAA.

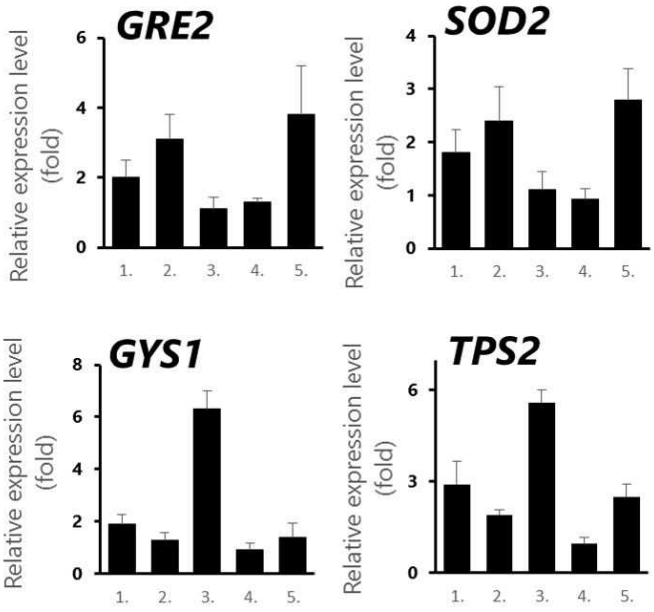

Fig. 9. Relative gene expression levels in each treatment condition. The relative expression levels were calculated by the comparative CT method. The *ACT1* gene was used as an endogenous control. 1. adsorbed fraction to TiO_2-NOAA under UV; 2. non-adsorbed fraction to TiO_2-NOAA under UV; 3. adsorbed fraction to TiO_2-NOAA without UV; 4. non-adsorbed fraction to TiO_2-NOAA without UV; 5. under UV.

Genes that were involved in the response to reserving energy sources were upregulated in the treatment conditions of TiO_2-NOAA adsorption Conditions 1 (*GSY1*; 1.9-fold, *TPS2*; 2.9-fold) and 3 (*GSY1*; 6.3-fold, *TPS2*; 5.6-fold). This result suggested that yeast cells that are adsorbed by TiO_2-NOAAs suffer stress that induced the synthesis of glycogen and trehalose. Comparing the result of Condition 1 with 3, it is possible that UV suppresses the level of stress that causes reserving energy sources. However, these stress responses are not critical compared to that by oxidative stress response.

2-2 *The effect of yttrium oxide nanoparticles on yeast cells*

2-2-1 INTRODUCTION

A nanoparticle is defined as a nano-object with all external dimensions in the nanoscale (length ranging from 1 to 100 nm), where the lengths of the longest and the shortest axes of the nano-object do not differ significantly (ISO/TS80004-2:2015http://www.iso.org/iso/home/store/catalogue_tc/catalogue_detail.htm?csnumber=54440)[13]. Among several types of nanoparticles currently in use, metal oxide nanoparticles constitute the bulk of commercially produced nanoparticles[14]. Despite the rapid progress and early acceptance of nanotechnology, the potential for adverse effects in humans and the environment has not yet been established.

Several studies exploring the cytotoxic effects of nanoparticles have been reported[15-19]. However, the findings are often specific to the laboratories where the study is carried out and have not been confirmed by other groups. Thus, there is a need to perform these evaluations under strictly controlled conditions. Recently, the International Standard Organization (ISO)/Technical Committee 229 (Nanotechnologies) published a document titled 'Nanotechnologies -- Characteristics of working suspensions of nano-objects for in vitro assays to evaluate inherent nano-object toxicity (ISO/TS19337:2016)[20]. The ISO/TS 19337 standard describes procedures to confirm 1) endotoxin content in the nanoparticles, 2) the stability of working suspensions, 3) the concentration of metal ions, and 4) the concentration of culture medium components. Endotoxins are contaminants derived from microbes that are known to cause cellular toxicity. Evaluating the stability of working suspensions that contain nanoparticles is another important issue, as the low stability of secondary structures obtained from original nano-objects and medium components can lead to low reproducibility[2]. Metal ion content in the working suspension is shown to be the main reason for toxicity of nanoparticles[14]. Medium components need to be measured accurately as nanoparticles have high absorbability.

Yttrium oxide (Y_2O_3) nanoparticles have widespread applications in various fields including biological imaging, photodynamic therapy, material sciences, and chemical synthesis of inorganic compounds[21]. However, toxicity due to

nanoparticles has also been reported[22, 23]. Previous studies have attributed this toxicity to the nano-structures. However, these evaluations were not performed according to ISO/TS 19337 standards and there is a need for a more accurate assessment. In this study, we evaluated the toxicity of yttrium oxide (Y_2O_3) nanoparticles as per ISO/TS 19337standard.

Saccharomyces cerevisiae was for this study, because this yeast is the most-studied eukaryotic model organism with characteristics well suited for bioassays. These include a relatively short life cycle, inexpensive growth culture requirements, and highly reproducible bioassay results[24]. It has been widely accepted that yeast is universally present in the environment and therefore, toxicogenomic results in yeast can be extrapolated for ecotoxicological purposes[25]. As per the ISO/TS 19337 standard, we evaluated the solubility of Y_2O_3 nanoparticles in yeast medium and found that the solubility was high. This suggests that the toxicity of Y_2O_3 nanoparticles is possibly is due to the yttrium ions. Consequently, we characterized the toxicity of both, Y_2O_3 nanoparticles and yttrium ions, and found that the toxicities share a common origin.

2-2-2 MATERIALS AND METHODS

2-2-2-1 Yeast strains and incubation conditions

S. cerevisiae strain S288C (IFO 1136 *MAT*a*SUC2 mal mel gal2 CUP1[cir+]*) was selected for this study. The cells were obtained during the exponential phase by incubating 50 µl of the pre-culture (5×10^6 cells) in 5 ml 2% yeast extract peptone dextrose (YPD) medium (2.0% Bacto™ peptone, 1% Bacto™ yeast extract; Becton Dickinson and Company, N.J., USA, and 2% d(+)-glucose; Wako Pure Chemical Industries, Osaka, Japan) at 30°C for 6 h.

Green fluorescent protein (GFP)-tagged *S. cerevisiae* BY4741 GFP-Pre3 (*MATa his3Δ1 leu2Δ0 met15Δ0 ura3Δ0 PRE3:GFP*(*S65T*)-*HIS3MX6*) and *S. cerevisiae* BY4741 GFP-Rpt6 (*MATa his3Δ1 leu2Δ0 met15Δ0 ura3Δ0 RPT6:GFP*(*S65T*)-*HIS3MX6)* were used for fluorescence spectroscopy. Briefly, 50 µl of the pre-culture (5×10^6 cells) was added to 5 ml of fresh YPD medium and incubated at 30°C for 6 h. Subsequently, 20 mg Y_2O_3 nanoparticles and 15 mg YCl_3 were added and incubated at 30°C for 2 h. Fluorescence was observed using a

System Microscope BX-53 (Olympus Corporation, Tokyo, Japan) (×400) with an exposure time of 1.5s.

2-2-2-2 Nanoparticles

The Y_2O_3 nanoparticles used in this study were obtained from CIK NanoTek Corporation (Tokyo, Japan). The primary particle size was 33 nm, with a specific surface area of 35 m^2/g, and purity of 99.9%. $YCl_3 \cdot 6H_2O$ (Wako Pure Chemical Industries, Osaka, Japan) soluble in Milli-Q water, was used as a control.

2-2-2-3 Spectrophotometric determination of yttrium ions with xylenol orange

Milli-Q water was used as the diluent to prepare 0.1 mM Xylenol Orange solution (XO-solution; Acros Organics, NJ, USA; molecular weight [MW]=716.62), 4 mM 1-hexadecylpyridinium bromide solution (CPB-solution; Kanto Chemical Co., Inc., Tokyo, Japan; MW=402.45), and 25 mM tris (hydroxymethyl) aminomethane (Tris-HCl) buffer solution (Kanto Chemical Co., Inc., Tokyo, Japan; MW=121.14). The pH of Tris-HCl was adjusted to 8.6 by adding HCl (Nacalai Tesque Incorporated, Kyoto, Japan) as a pH regulator. Y_2O_3 nanoparticles (3, 10, and 20 mg) were added to 5 ml of 2% YPD broth. After incubation for 2 h with shaking, the mixture was centrifuged at 13000 rpm for 10 min. The supernatant (100 μl) was mixed with 900 μl of a detection reagent (50% Tris-HCl buffer, 37.5% XO-solution, 12.5% CPB-solution), and the absorbance was measured at 600 nm.

2-2-2-4 RNA extraction

The yeast cells were grown to anaphase of the logarithmic growth cycle (6-h culture) and collected by centrifugation at 15000 rpm for 1 min at 4°C (MX-301; Tomy Seiko, Tokyo, Japan). Total RNA was extracted by using the phenol-chloroform method with a Fast RNA® Pro Red Kit (MP Biomedicals, California, USA) according to the manufacturer instructions, with the following modification: cell disruption was performed for 10 min using a Multi-Beads Shocker® (Yasui Kikai, Osaka, Japan). Total RNA was purified using the RNeasy® Mini Kit (Qiagen, Hilden, Germany) according to the manufacturer instructions. The concentration and purity of the resulting RNA were evaluated by absorbance at

260 nm using an Agilent 2100 Bioanalyzer™ (Agilent Technologies, California, USA).

2-2-2-5 Real Time RT-PCR

The total RNA extracted from yeast as described above was subjected to reverse transcription at 37°C for 15 min using a ReverTra Ace® qPCR RT Master Mix (Toyobo, Osaka, Japan). The resulting cDNA was used for quantitative polymerase chain reaction (PCR) using the Power SYBR® Green Master Mix (Applied Biosystems, Calif., USA) and the StepOnePlus™ real-time PCR System (Applied Biosystems), according to the manufacturer's instructions. The themal cycling was carried out as follows: holding at 95°C for 10 min, and 40 cycles of the following: denaturation at 95°C for 15 s, annealing and extension at 60°C for 2 min. The relative expression levels were calculated from Ct values. Five pairs of primers were designed for this study (Table 3) using Primer3Plus software (http:/www.bioinformatics.nl/cgibin/primer3plus/primer3plus.cgi/).

Table 3. Sequences of oligonucleotide primers used in this study.

Experiment	**Gene name**	**F-primer**	**R-primer**
Conditions for Y_2O_3 nanoparticle treatment	*MET17*	CGCTCAAACCCTTGCCATCCA	TGACAGAAGTAACCACCGGCACCA
	SAM2	CAGATATCGCTCAAGGTCTGC	GGTAACCCTTCTGGAGTTTCG
	OPI3	TGGGGCCAGAAAGGGCTGTT	AGCCCGGCAGGCTTTGGTTT
Quantitative assessment	*RPN4*	ACTAGTGAAGCAACGGCCAA	CTTCTGCAATGGGGTTTCGC
	RPL30	TGCCGCTAACACTCCAGTTT	ACCGACAGCAGTACCCAATT
Endogenous control	*ACT1*	ATTGCCGAAAGAATGCAAAAGG	CGCACAAAACAGAGATTAGAAACA

2-2-2-6 DNA microarray

The DNA probes used in the microarray corresponded to 6256 genes of *S. cerevisiae* strain S288C. Complementary DNA was prepared from total RNA using a Quick Amp Labeling Kit^{TM} (Agilent Technologies, CA, USA). Complementary RNA that was fluorescently labeled with cyanine 3-cytidine triphosphate (CTP)- was amplified from cDNA using T7 RNA polymerase (Agilent Technologies, CA, USA). The CTP-labeled cRNA was used for hybridization to Yeast (V2) Gene Expression Microarray slides (#G4813A016322, Agilent Technologies, CA, USA) at 65°C for 17 h. The hybridized microarray slides were washed according to the manufacturer's instructions and scanned using an Agilent DNA Microarray Scanner (#G2565CA, Agilent Technologies, CA, USA) at a resolution of 5 μm. The scanned images were analyzed quantitatively using Agilent Feature Extraction Software version 10.7.3.1 (Agilent Technologies, CA, USA). Signals detected from each open reading frame (ORF) were normalized using the quantile methods[26]. The genes classified as up-regulated or down-regulated were those that passed the Student's *t*-test ($P < 0.05$). Ratios of the hybridization intensity (treatment/control) > 2.0 indicated up-regulation and those <0.5 indicated down-regulation.

The gene-expression profiles were characterized according to the categories of the Database for Annotation, Visualization and Integrated Discovery (DAVID, https://david.ncifcrf.gov/) and the *Saccharomyces* Genome Database (SGD, http://www.yeastgenome.org/). The DNA microarray experiments described in this study are MIAME compliant and the raw data have been deposited in the Gene Expression Omnibus (GEO) database under the accession number GSE80677.

2-2-3 RESULTS AND DISCUSSION

2-2-3-1 Solubility of yttrium oxide nanoparticle

Several previous studies have demonstrated that Y_2O_3 nanoparticles have detrimental effects on various organisms[22, 23]. However, those evaluations have not considered the solubility of Y_2O_3 nanoparticles. In this study, we evaluated the solubility of Y_2O_3 nanoparticle in YPD medium, based on the ISO/TS 19337 technical standard. The solubility of the nanoparticles was directly proportional to the concentration of yttrium ions (Fig 10).

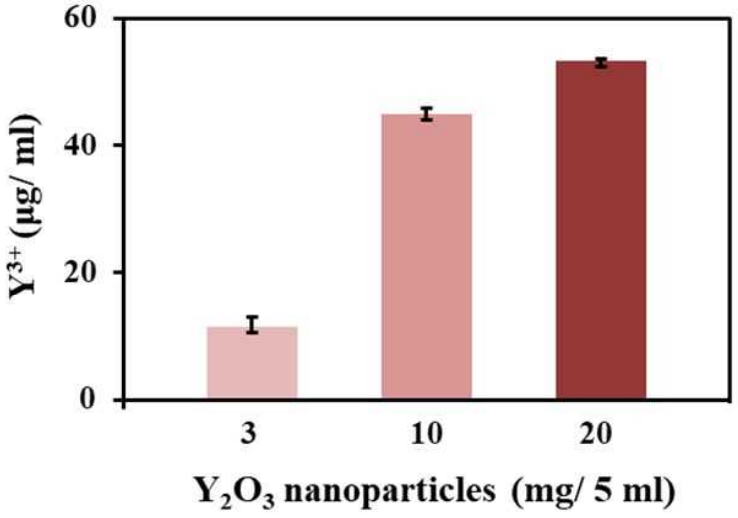

Fig.10. Measurement of solubility of Y_2O_3 nanoparticles in YPD broth.Y_2O_3 nanoparticles were added at concentrations of 3, 10, and 20 mg in 5 ml 2% YPD medium and shaken for 2 h. Absorbance was measured at 600 nm.

2-2-3-2 Induction of genes by treatment with yttrium oxide nanoparticle conditions corresponding to IC50

We have previously collected transcriptome data in response to stress conditions, using IC50 conditions obtained by comparing the growth rate without stress conditions[24]. Growth rate can be monitored by measuring absorbance or the number of colony-forming units (CFU). The treatment conditions were determined by using IC50 values based on CFU (YCl_3: 5 mg/5 ml, Y_2O_3 nanoparticles: 3 mg/5 ml).

Gene expression after YCl_3 treatment was confirmed by DNA microarray analysis. The results showed that 402 genes were induced more than 2.0-fold (P <0.05) and 206 genes were repressed less than 0.5-fold ($P < 0.05$). On the other hand, in treatment with Y_2O_3 nanoparticles, only 9 genes were induced more than 2.0-fold (P<0.05) and 27 genes were repressed less than 0.5-fold (P<0.05).

The results defining 3 mg/5 ml of Y_2O_3 nanoparticles as the IC50 value indicated minimal level of stress to yeast cells. We further explored for the cause for minimal stress caused by the Y_2O_3 nanoparticles under IC50 conditions and detected

adsorption of yeast cells onto Y_2O_3 nanoparticles. Some yeast cells that were adsorbed onto Y_2O_3 nanoparticles or the resultant nano-objects, their aggregates, and agglomerates (NOAA) that were >100 nm in size produced a single colony on the agar plate and therefore, the CFU was reduced without lower level of stress (Fig. 11).

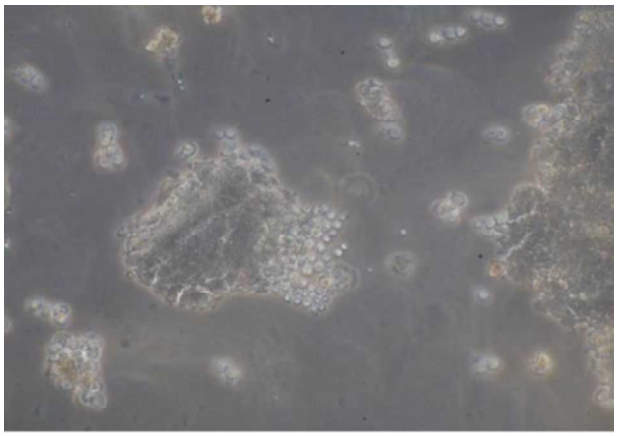

Fig. 11. Adsorption of yeast cells by Y_2O_3 nanoparticles.To determine adsorption of yeast cells into the nanoparticles, 50 μl of pre-culture (5×10^6 cells) was added to 5 ml of fresh YPD medium and incubated at 30°C for 6 h. Subsequently, 20 mg Y_2O_3 nanoparticles and 15 mg YCl_3 were added and incubated at 30°C for 2 h. Fluorescence was observed using System Microscope BX-53 (Olympus Corporation, Tokyo, Japan) (×400).

2-2-3-3 Transcriptomics conditions for the yttrium oxide nanoparticle treatment.

Alternatively, gene expression level can be used as a marker to identify appropriate Y_2O_3 treatment conditions. In the case of YCl_3 (5 mg/5 ml) treatment, the genes related to oxidative stress were significantly up-regulated. Of these, 3 genes (*MET17*, *SAM2*, *OPI3*) were selected based on their fold increase and expression levels (Table 4). If the toxicity caused by yttrium oxide nanoparticles is due to yttrium ions, then it is necessary to identify the conditions created by yttrium oxide nanoparticles that induce these genes. We identified the conditions under which yeast cells significantly expressed these genes after treatment with Y_2O_3 nanoparticles. We treated the yeast cells with 3, 10, and 20 mg/5 ml of nanoparticle suspentions. The treatment with 20 mg/5 ml Y_2O_3 nanoparticles, showed 3 genes

with a significant fold increase (*MET17*: 4.3-fold, *SAM2*: 3.1-fold, *OPI3*: 12-fold, Table 5) and these expression levels were similar to those obtained with 5 mg/5 ml YCl_3. This result showed that yeast cells suffer stress after treatment with Y_2O_3 nanoparticles (20 mg/5 ml) to a similar degree as that caused by 5 mg/5 ml YCl_3. Therefore, the concentration of Y_2O_3 nanoparticles was selected as 20 mg/5 ml. Based on gene expression levels, we selected 20 mg/5 ml Y_2O_3 conditions for transcriptome analysis.

Table 4. List of genes highly induced in yeast cells by YCl_3 treatment.

Gene name	Expression levels		Fold
	Control	YCl_3-treatment	(YCl_3/C)
OPI3	18254	117344	6.43
SAM2	8664	55366	6.39
MET17	12644	76212	6.03
LEU2	5133	21864	4.26
GDH1	6497	24485	3.77
SER3	5087	16860	3.31
SAM1	18087	56059	3.10
ITR1	14918	45988	3.08
LYS9	12130	36271	2.99
HXT4	12662	37236	2.94
PSD1	5370	15571	2.90
RNR4	16738	48204	2.88
PYC1	6549	18849	2.88
GOR1	5843	16540	2.83
LYS4	8174	22797	2.79
HNM1	12250	31945	2.61
CHO1	14183	36054	2.54
HOM3	5214	13237	2.54
RNR1	10028	24727	2.47
FCY2	19299	47277	2.45
HXT3	24750	59418	2.40
MOG1	5792	13626	2.35
NSR1	28051	65334	2.33
RNR2	48364	110902	2.29

APE1	26190	59214	2.26
DIC1	5845	13140	2.25
LYS20	10453	23419	2.24
OLE1	14916	32845	2.20
COT1	5632	12322	2.19
LYS21	10227	22276	2.18
EHT1	9860	21476	2.18
ILV5	13444	29208	2.17
LEU4	23892	50847	2.13
FRD1	11839	24218	2.05
BNA3	6994	14048	2.01

Table 5 Relative gene expression levels after treatment with either Y_2O_3 nanoparticles or YCl_3.

Gene name	**Relative expression levels expression levels**				
	Control	Y_2O_3 nano /5 ml			YCl_3/5 ml
		3 mg	10 mg	20 mg	5 mg
MET17	1.0	1.4 ± 0.55	1.7 ± 0.57	4.3 ± 0.49	2.1 ± 1.1
SAM2	1.0	1.0 ± 0.54	1.4 ± 0.53	3.1 ± 1.1	2.2 ± 0.45
OPI3	1.0	1.6 ± 0.19	7.9 ± 2.1	12 ± 0.93	8.7 ± 4.1

2-2-3-4 Transcriptome analysis of genes induced by treatment with 20 mg/5 ml Y_2O_3 nanoparticles

We performed yeast DNA microarray analysis using 6256 ORF probes. The 20 mg/5 ml Y_2O_3 condition caused an alteration in 4754 out of 6256 ORFs, as determined by the Student's *t*-test ($P < 0.05$). This value is much higher than our previous results. Among these altered genes, 1157 ORFs were up-regulated > 2-fold than control, and 1212 ORFs were down-regulated < 0.5-fold than control.

The 1157 ORFs up-regulated in cells treated with 20 mg/5 ml Y_2O_3 nanoparticles were classified based on functional category by using the DAVID tool suite (2016/11/16 https://david.ncifcrf.gov/summary.jsp). Using DAVID, we may evaluate the induced or repressed functions according to functional information of each gene. The functions of

the up-regulated genes were classified with high probability into categories of "Oxidoreductase (40.4%)", "Stress response (41.7%)", "NADP/ NAD (38.6%/ 35.2%)", "Methionine biosynthesis (38.6%)", "Proteasome (46.2%)", and "Peroxisome (37.7%)" (Table 6). The genes related to "oxidoreductase" were also up-regulated by 5 mg/5 ml YCl_3 treatment (16.1%, Table 7), oxidative stress was considered to be common in both treatments: 20 mg/5 ml Y_2O_3 and 5 mg/5 ml YCl_3. However, it should be noted that Y_2O_3 treatment significantly induced proteasome-related genes (e.g. RPN4; 9.24-fold, Table 8), which was not observed with YCl_3.

Table 6. Functional annotation of up-regulated genes after treatment with 20 mg/5 ml Y_2O_3 nanoparticles.

Functional annotation	Number of total genes	Number of altered genes	Percentage of altered gene (%)	*P*value
Oxidoreductase	255	103	40.4	7.E-21
Stress response	84	35	41.7	7.E-08
NADP	83	32	38.6	2.E-06
Methionine biosynthesis	27	15	55.6	2.E-05
NAD	88	31	35.2	3.E-05
Sporulation	94	32	34.0	4.E-05
Proteasome	39	18	46.2	5.E-05
Stress-induced protein	17	11	64.7	8.E-05
Respiratory chain	27	14	51.9	1.E-04
Autophagy	35	16	45.7	2.E-04
Peroxisome	53	20	37.7	4.E-04
Heat shock	17	10	58.8	5.E-04
Ubl conjugation pathway	130	37	28.5	6.E-04
Oxidative phosphorylation	28	13	46.4	7.E-04
Tricarboxylic acid cycle	28	13	46.4	7.E-04

Table 7. Functional annotation of up-regulated genes after treatment with 5 mg/5 ml YCl_3

Functional annotation	Number of total genes	Number of altered genes	Percentage of altered gene (%)	*P*value
Amino-acid biosynthesis	97	32	33.0	4.E-16
Oxidoreductase	255	41	16.1	2.E-09
Methionine biosynthesis	27	13	48.1	7.E-09
NADP	83	18	21.7	3.E-06
Amino-acid transport	35	11	31.4	2.E-05
Transport	788	72	9.1	3.E-05
Purine metabolism	5	5	100.0	5.E-05
Arginine biosynthesis	9	6	66.7	6.E-05
Lysine biosynthesis	9	6	66.7	6.E-05
Transmembrane	1401	111	7.9	7.E-05
Lyase	74	14	18.9	2.E-04
Cysteine biosynthesis	12	6	50.0	3.E-04
Transmembrane protein	1566	118	7.5	3.E-04
Iron	107	16	15.0	9.E-04
Homotetramer	15	6	40.0	1.E-03

Table 8. Dominant genes related to “proteasome”, as classified by DAVID.

Functional annotation	Gene name	Fold [Y_2O_3/control]	Fold [YCl_3/control]	Description
proteasome	PRE5	2.08	1.18	Alpha 6 subunit of the 20S proteasome
	PRE6	2.01	0.86	Alpha 4 subunit of the 20S proteasome
	PUP3	2.31	1.32	Beta 3 subunit of the 20S proteasome
	RPN4	9.24	0.85	Transcription factor that stimulates expression of proteasome genes
	NAS2	2.32	0.68	Proteasome-interacting protein
	UMP1	3.25	0.79	Chaperone required for correct maturation of the 20S proteasome

2-2-3-5 Transcriptome analysis of genes repressed due to treatment with 20 mg/5 ml Y_2O_3 nanoparticles

We analyzed 1212 ORFs down-regulated by 20 mg/5 ml Y_2O_3 nanoparticles. Using DAVID, we found that a significant number of down-regulated genes were involved in "Protein biosynthesis" (66.9%, e.g. RPL36A; 0.13-fold, RPL1A; 0.18-fold) and "Ribosome biogenesis" (84.5%, e.g. RRB1; 0.14-fold, RPB5; 0.25-fold) (Table 9, 11). After YCl_3 treatment, the genes related to "Protein biosynthesis" (e.g. RPL36A; 0.81-fold, RPL30; 0.90-fold) and "Ribosome biogenesis" (RRB1; 1.36-fold, RPL15A; 0.90-fold) were repressed to a lesser extent than that caused by Y_2O_3 nanoparticle treatment (Table 10, 11).

Table 9. Functional annotation of down-regulated genes after treatment with 20 mg/5 ml Y_2O_3 nanoparticles.

Functional annotation	Number of total genes	Number of altered genes	Percentage of altered gene (%)	*P*value
Protein biosynthesis	257	172	66.9	1.E-71
Ribosome biogenesis	148	125	84.5	1.E-71
Ribonucleoprotein	280	165	58.9	6.E-57
Ribosome	156	112	71.8	8.E-51
rRNA processing	155	107	69.0	7.E-46
Ribosomal protein	195	119	61.0	9.E-43
Cytosol	72	55	76.4	6.E-27
Phosphoprotein	2618	602	23.0	3.E-22
Cytoplasm	1397	357	25.6	2.E-18
Initiation factor	29	25	86.2	2.E-14
Acetylation	164	68	41.5	7.E-13
Nucleus	1636	374	22.9	6.E-11
Amino-acid biosynthesis	97	44	45.4	5.E-10
RNA-binding	300	96	32.0	5.E-10
rRNA-binding	20	16	80.0	2.E-08

Table 10. Functional annotation of down-regulated genes after treatment with 5 mg/5 ml YCl_3.

Functional annotation	Number of total genes	Number of altered genes	Percentage of altered gene (%)	*P*value
Amino-acid transport	35	8	22.9	6.E-05
Amino acid transport	8	4	50.0	1.E-03
Stress response	84	9	10.7	3.E-03
Peptide transport	4	3	75.0	5.E-03
Heat shock	17	4	23.5	1.E-02
Stress-induced protein	17	4	23.5	1.E-02
Phosphoric monoester hydrolase	37	5	13.5	2.E-02
Aminotransferase	22	4	18.2	3.E-02
Copper transport	9	3	33.3	3.E-02
Phosphohistidine	10	3	30.0	3.E-02
Iron	107	8	7.5	4.E-02
Iron transport	26	4	15.4	4.E-02
Pyridoxal phosphate	47	5	10.6	5.E-02
Transport	788	32	4.1	5.E-02
Cell membrane	196	11	5.6	6.E-02

Table 11. Dominant genes related to "Protein biosynthesis" and "Ribosome biogenesis," as classified by DAVID.

Functional annotation	Gene name	Fold [Y_2O_3 nano/Control]	Fold [YCl_3/Control]	Description
Protein biosynthesis	*RPS8B*	0.07	0.68	Protein component of the small (40S) ribosomal
	RPL36A	0.13	0.81	Ribosomal 60S subunit protein L36A
	RPL1A	0.18	0.74	Ribosomal 60S subunit protein L1A
	RPL30	0.11	0.90	Ribosomal 60S subunit protein L30
Ribosome biogenesis	*SSF1*	0.21	1.98	Constituent of 66S pre-ribosomal particles
	RRB1	0.14	1.36	Specific chaperone for ribosomal protein Rpl3p
	RPB5	0.25	0.70	RNA polymerase subunit ABC27
	RPL15A	0.43	0.90	Ribosomal 60S subunit protein L15A

2-2-3-6 Induction of "Proteasome"-related genes by YCl_3 treatment

DNA microarray analysis revealed that the functional group of "Proteasome" is specifically induced by treatment with 20 mg/5 ml Y_2O_3 nanoparticles. After YCl_3 treatment, the genes related to "Protein biosynthesis" and "Ribosome biogenesis" were less repressed compared to that after Y_2O_3 nanoparticle treatment. Therefore, we increased YCl_3 concentration. The yeast cells were treated with 5, 10, and 15 mg/5 ml concentrations. Table 11 summarizes the expression levels of RPN4, a proteasome-related gene and those of RPL30, a key gene for protein synthesis. As the concentration of YCl_3 increased, the proteasome-related gene was up-regulated (15 mg/5 ml: 17-fold), while the protein synthesis-related gene was down-regulated (15 mg/5 ml: 0.11-fold) (Table 12).

The proteasome is a cellular organelle that can be directly monitored. In this study, we visualized the proteasome of *S. cerevisiae* BY4741 strains, GFP-Pre3 and GFP-Rpt6 after treatment with 20 mg/5 ml Y_2O_3 nanoparticles and 15 mg/5 ml YCl_3. Prior to treatment, the yeast cells showed low-intensity green color, probably corresponding to the proteasome. After the yeast cells were cultured for 6 h, they were treated with 20 mg Y_2O_3 nanoparticles and 15 mg YCl_3, and then incubated at 30°C for 2 h. Both of strains showed significant green structures (Fig. 12). Thus, we confirmed the clear appearance of proteasome structures after Y_2O_3 nanoparticle and YCl_3 stress conditions.

Table 12. Relative gene expression levels in each treatment condition.

	Relative expression level (fold)			
Gene name		YCl_3 mg/5 ml		
	Control	5 mg	10 mg	15 mg
RPN4	1.0	3.9 ± 0.79	14 ± 1.4	17 ± 3.9
RPL30	1.0	0.25 ± 0.019	0.046 ± 0.00046	0.099 ± 0.013

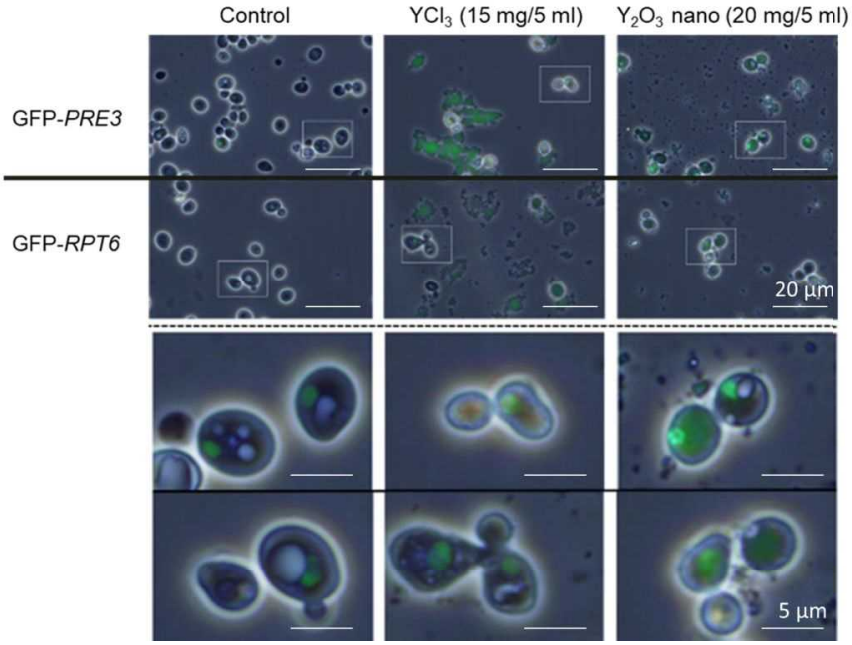

Fig. 12. Fluorescent observation of GFP-tagged yeast cells.

Green fluorescent protein (GFP)-tagged *S. cerevisiae* BY4741 GFP-Pre3 (MATa his3Δ1 leu2Δ0 met15Δ0 ura3Δ0 PRE3:GFP (S65T)-HIS3MX6) and *S. cerevisiae* BY4741 GFP-Rpt6 (MATa his3Δ1 leu2Δ0 met15Δ0 ura3Δ0 RPT6:GFP(S65T)-HIS3MX6) were used for fluorescence spectroscopy. Briefly, 50 µl of pre-culture (5×10^6 cells) was added to 5 ml of fresh YPD medium and incubated at 30°C for 6 h. Subsequently, 20 mg Y_2O_3 nanoparticles and 15 mg YCl_3 were added and incubated at 30°C for 2 h. Fluorescence was observed using a System Microscope BX-53 (Olympus Corporation, Tokyo, Japan) with exposure time of 1.5 s. Treatment with YCl_3 and Y_2O_3 nanoparticles increased fluorescence of both groups of GFP-tagged yeast cells

Several studies have shown that Y_2O_3 nanoparticles have detrimental effects on various organisms. However, these evaluations did not considered the solubility of the Y_2O_3 nanoparticle. Therefore, we evaluated the solubility of Y_2O_3 nanoparticle in YPD medium and concluded that the effect of Y_2O_3 nanoparticle can be attributed to release of yttrium ions.

ISO/TS 19337 includes the consideration of the possibility high absorbability of nanoparticles and this characteristic gave the illusion of IC50. We found that some yeast cells that were adsorbed onto Y_2O_3 nanoparticles or the NOAA. In

generaly one cell makes one colony, but some yeast cells adsorbed on nanoparticle also seem to make one colony. This finding showed probably effecting that the CFU was reduced due to not stress but adsorbability. This result suggests that the evaluation of IC50 in terms of CFU is not useful when treating yeast cells with yttrium oxide nanoparticles and other nano-objects. This aggregation can be the main reason for the illusion of antibacterial activity.

Lin *et al.* estimated the cell viability of *E. coli* upon exposure to TiO_2 nanoparticles (TiO_2NPs) through the colony count assay[27]. They investigated the toxicities of five types of TiO_2 NPs with different particles sizes (10~50 nm) and crystal phases and reported that a marked particle size and crystal phase dependent nanotoxicity were observed. However, they did not confirm whether the aggregation decreased CFU. Zhang *et al*. also reported he antibacterial activity of graphene oxide (GO) on *E. coli*[28]. They showed that with increasing concentrations of GO, the viability of *E. coli* decreases. They suggested that the antibacterial mechanism of GO results from the membrane destruction and oxidative stress. They shook tubes containing *E. coli* and GO with 250 rpm in sterile saline water. This may cause physical damages by colliding aggregates of microbes and GO. In addition, the incubation of *E. coli* in sterile saline water can be the starvation stress but no such controls were evaluated.

He *et al.* reported the antibacterial activity of GO nanosheets against common dental pathogens, such as *S. mutans*, *P. gingivalis* and *F. nucleatum*[29]. In thier study, the antibacterial activity was also estimated by the CFU counting method. Through this method, GO nanosheets have severe antibacterial activity for microbes. It is easy to image the attached microbes onto the sheets.

It is strongly required for those reports to confirm that decreased viability did not result from aggregation of nanoparticles and microbes. Therefore, we set a new treatment concentration of Y_2O_3 nanoparticles (20 mg/5 ml) for interaction with yeast cells at a similar degree as that by 5 mg/5 ml YCl_3. It was also decided to base the analysis on gene expression levels.

Next, we performed yeast DNA microarray experiments with the new treatment concentration of Y_2O_3 nanoparticles (20 mg/5 ml).The up-regulated genes involved in "Oxidoreductase," "NADP," and "NAD" are implicated in the redox reaction and repair

of oxidative damage [30, 31]. Additionally, methionine is a sulfur-containing amino acid and relevant to oxidative response[32, 33]. This result suggests that yeast cells suffer oxidative stress. Moreover, Michael Schrader *et al.* reported that peroxisomes are not just considered as a source of oxidative stress, but also can respond to oxidative stress and reactive oxygen species generated either intra- or extracellularly[34]. Therefore, the up-regulation of genes related to "Peroxisome" supports oxidative stress in yeast cells under Y_2O_3 nanoparticle-treatment conditions. The oxidative stress was considered to be common in both treatments: 20 mg/5 ml Y_2O_3 and 5 mg/5 ml YCl_3.

In contrast, only the YCl_3 treatment significantly induced proteasome-related genes. The down-regulated genes were classified with high probability into categories of "Protein biosynthesis". It has been reported that genes involved in protein synthesis are down-regulated in response to diverse environmental stress conditions[11]. Therefore, this result suggests that yeast cells treated with 20 mg/5 ml Y_2O_3 nanoparticles were significantly stressed. Table 6 and 7 show that the induction functions are almost similar in 20 mg/5 mL Y_2O_3 nanoparticles treatment and 5 mg/5 mL YCl_3 treatment, but the function related to proteasome was induced in 20 mg/5 mL Y_2O_3 nanoparticles treatment. In Table 9 and 10, it is shown that 20 mg/5 mL Y_2O_3 nanoparticles treatment was a stronger stress induction than 5 mg/5 mL YCl_3 treatment, because suppression of RNA metabolism-related functions is more prominent.

DNA microarray analysis revealed that the functional group of "Proteasome" is specifically induced by treatment with 20 mg/5 ml Y_2O_3 nanoparticles. Two possibilities can be considered here: either Y_2O_3 nanoparticles specifically induce this function or YCl_3 (5 mg/5 ml) treatment does not have this effect. According to the transcriptome analysis of genes repressed by treatment with Y_2O_3 nanoparticles and YCl_3, the conditions created by YCl_3 treatment for yeast cells were weaker than that by Y_2O_3 nanoparticle treatment. To confirm this possibility, we increased YCl_3 concentration. As the concentration of YCl_3 increased, we confirmed that the proteasome-related gene was up-regulated, while the protein synthesis-related gene was down-regulated, and the clear appearance of proteasome structures after Y_2O_3 nanoparticle and YCl_3 stress conditions (Fig. 12). This phenomenon also showed and clarified that the conditions created by YCl_3 treatment (5 mg/5 ml) were mild

compared to those created by Y_2O_3 nanoparticle treatment (20 mg/5 ml).

We carried out a catch ball analysis of yttrium oxide and yttrium ion toxicities. The results indicated that yeast cells undergo oxidative stress (up-regulated genes related to “Oxidoreductase”, “NADP”, Table6, 7) after Y_2O_3 nanoparticle (20 mg/5 ml) and YCl_3 (5 mg/5 ml) treatment.

These results suggest that Y_2O_3 nanoparticle and YCl_3 share similar toxicity effects and therefore, the toxicity caused by Y_2O_3 nanoparticle is due to yttrium ions. In the medium, Y^{3+} ions immediately precipitated with a medium component and the toxicity was caused by minor part of solubilized Y^{3+} ions. It has been reported that heavy metal ions impede protein folding and promote protein aggregation[35]. We assumed that proteasome formation may be induced by the accumulation of denatured proteins caused by interactions between yttrium ions and protein.

Thus far there is no regulatory control for yttrium release into the environment. Given the increasing of amount of used and flow-out for environment, a new control is thought to be necessary. Yttrium nanoparticles do induce oxidative stress that is often associated with that caused by heavy metal ions such as Cd[8] and Cu[36]. Thus, the use of yttrium nanoparticles or yttrium ion must be controlled like heavy metals.

2-3 *Assessment of biological effects of recyclable carbon fiber*

2-3-1 INTRODUCTION

Carbon fibers are used in the manufacture of aircraft and automobiles, and their production is increasing year by year. Gifu Prefecture and Gifu University are developing technologies for recycling used carbon fibers because of the high cost and energy required for their disposal. In this recycling method, generation of carbon fiber dust was found to be a serious concern, especially in the occupational environment. The demand for CFRP is expected to grow in the future, and the possibilities for its exposure to the general society and concern about its effects on their health will also increase. So, it is necessary to study the effect of carbon fibers (on the order of nm-μm) on human health at the molecular level. Recent in vitro studies have highlighted the cytotoxicity of MWCNTs in human lung or bronchial epithelial cell culture systems[37-39]. Therefore, it is necessary to evaluate the biological effect of recycled carbon fiber before it is used at the industrial scale. In this study, we investigated three types of carbon fiber dust - before recycling (Virgin Carbon fiber; VCF), after carbonization (Carbonized Carbon fiber; CCF), and after firing (Recycled Carbon fiber; RCF). Suspensions of these carbon fiber dusts were administered by intratracheal and intraperitoneal instillation in mice (2.0 mg per mouse). After 30, 90, and 180 days, pathological analyses were conducted on the lungs and liver. There are numerous toxicity reports on fibrous materials (including asbestos and CNTs). Intratracheal instillation is a general method to assess the lung effects of nanomaterials. Intraperitoneal instillation is not very general method, but it is a highly sensitive test. We also selected this dosing method as a test of whether carbon fiber could meet this safety criterion for animals. Some researchers have previously reported that toxicity depends on fiber length[40, 41], while others have reported that it depends on diameter and rigidity[42]. The detailed mechanisms are still unknown.

In this work, we studied the toxicity of carbon fibers produced during the recycling process so that needless concern regarding human health may be averted in the future and defensive action plans can be devised. Ascertaining the toxicity mechanisms is also of interest.

2-3-2 MATERIALS AND METHODS

2-3-2-1Test materials

Three types of carbon fibers (CFs) (before recycling, VCF; after carbonization, CCF; and after firing, RCF) were obtained from Carbon Fiber Recycle Industry Co., Ltd. (Gifu, Japan). CFs were collected and filtered through a membrane filter (40-μm pore size) using an Andersen stack sampler (TOKYO DYLEC Co., Ltd., Tokyo, Japan). Carbonized CF was first heat-treated at 500 °C for 180 min, then further heat-treated at 400 °C for 180 min, and designated as Recycled CF. Carbon fibers were suspended in PBS (4.0 mg/mL). 50 μL of each material suspension was intratracheally or intraperitoneally instilled once in mice (200 μg fiber per mouse).

2-3-2-2 Animals

Eight-week-old male C57BL/6N mice were purchased from Charles River Laboratories Japan. Carbon fibers were intratracheally or intraperitoneally administered into mice in a single injection (0.2 mg fiber per mouse). PBS was administered to the vehicle control groups. The mice were stratified into following: 1 month -intratracheal instillation; control; n=6, VCF; n=6, CCF; n=6, RCF; n=8, 6 months -intratracheal instillation; control; n=8, VCF; n=6, CCF; n=9, RCF; n=8, intraperitoneal instillation; control; n=6 (n = 2 after 1 month-post instillation), VCF; n=4, CCF; n=4, RCF; n=4. After instillation treatment, the mice were housed within polycarbonate cages at a controlled temperature of 22 °C with a chow diet ad libitum. The intratracheal administered mice were dissected at 1 or 6 months post-instillation, whereas the intraperitoneally administered mice were dissected at 90 days post-instillation. The lungs of anesthetized mice were perfused with physiological saline, excised, and subjected to morphological observation, histopathological findings, and comprehensive gene expression microarray analysis (Intratracheal instillation). The animal experiment committee of Gifu University approved these animal experiments (15044 and 16079).

2-3-2-3 Histopathological analysis

After the mice were sacrificed, their left lungs were rapidly removed and processed for histopathological findings or biochemical analysis. Next, lung tissues were fixed in 4% buffered paraformaldehyde, followed by embedding in paraffin, and

the sections were stained with hematoxylin and eosin stain.

2-3-2-4 RNA extraction

Right lungs were homogenized using disposable homogenizer (BioMasher®, Nippi, Tokyo, Japan). Total RNA was extracted by phenol-chloroform method using a Fast RNA® Pro Red Kit (MP Biomedicals, California, USA) following the manufacturer's instructions. Total RNA was purified using RNeasy® Mini Kit (Qiagen, Hilden, Germany) according to the manufacturer instructions. The concentration and purity of the resulting RNA were evaluated by absorbance at 260 nm using an Agilent 2100 BioanalyzerTM (Agilent Technologies, California, USA).

2-3-2-5 DNA microarray analysis

Complementary DNA was prepared from total RNA using a Quick Amp Labeling KitTM (Agilent Technologies, CA, USA). Complementary RNA that was fluorescently labeled with cyanine 3-cytidine triphosphate (CTP)- was amplified from cDNA using T7 RNA polymerase (Agilent Technologies, CA, USA). The CTP-labeled cRNA was used for hybridization to Whole Mouse Genome Kit 4x44K or SurePrint G3 Mouse Gene Exp v2 Array kit Microarray slides (#G4122-60520 and #G4852-60520, Agilent Technologies, CA, USA) at 65°C for 17h. The hybridized microarray slides were washed according to the manufacturer instructions and scanned using an Agilent DNA Microarray Scanner (#G2565CA, Agilent Technologies, CA, USA) at a resolution of 5 μm. The scanned images were analyzed quantitatively using Agilent Feature Extraction Software version 10.7.3.1 (Agilent Technologies, CA, USA).

Normalized data were analyzed using GeneSpring GX version 11.5.1 software (Agilent Technologies). The genes classified as up-regulated or down-regulated were those that passed the Student's t-test ($P < 0.05$). Ratios of the hybridization intensity (treatment/control) > 2.0 were considered up-regulated and those <0.5 were considered down-regulated. Gene expression data for each experimental group were deposited into the Gene Expression Omnibus database (Accession number GSE130496 and GSE130497; https://www.ncbi.nlm.nih.gov/geo/).The gene-expression profiles were characterized according to the categories of the Database for Annotation, Visualization and Integrated Discovery (DAVID, https://david.ncifcrf.gov/).

2-3-2-6 Real-time qPCR

The RNA used for DNA microarray analysis was subjected to reverse transcription (RT) at 37 °C for 15 min using a ReverTra Ace® qPCR RT Master Mix (Toyobo, Osaka, Japan). For quantitative PCR amplification, Power SYBR® Green Master Mix (Applied Biosystems, CA, USA) and StepOnePlus™ real-time PCR System (Applied Biosystems) were used, as described in the manufacturer's instructions (holding at 95 °C for 10 min, followed by 40 cycles of denaturation at 95 °C for 15 s, and annealing and extension at 60 °C for 2 min). The primers of qPCR are described in Table 13. Results were calculated using the relative $2^{-\Delta\Delta Ct}$ method[43]. All expression data were normalized to endogenous control Gapdh expression.

Table 13 Primers for amplification of the listed genes by real-time PCR.

Gene	Forward (5' to 3')	Reverse (5' to 3')
Hba-a1	TGCCTCTCTGGACAAATTCC	CAGGTGCAAGGGAGAGAAGA
Hba-a2	GAAGCCCTGGAAAGGATGTT	GCCGTGGCTTACATCAAAGT
Hbb-b1	TGCATGTGGATCCTGAGAAC	GTGAAATCCTTGCCCAGGT
Gapdh	ACTGGCATGGCCTTCCG	CAGGCGGCACGTCAGATC

2-3-2-7 Statistical analysis

All numerical values are represented as the mean±S.E. Statistically significant differences between the data for the treated samples and the untreated controls were determined using Student's t-test.

2-3-3 RESULTS AND DISCUSSION

2-3-3-1 Body weight and general condition

We used three different types of carbon fiber (Fig. 13): before recycling, VCF; after carbonization, CCF; and after firing, RCF were from Carbon Fiber Recycle Industry.

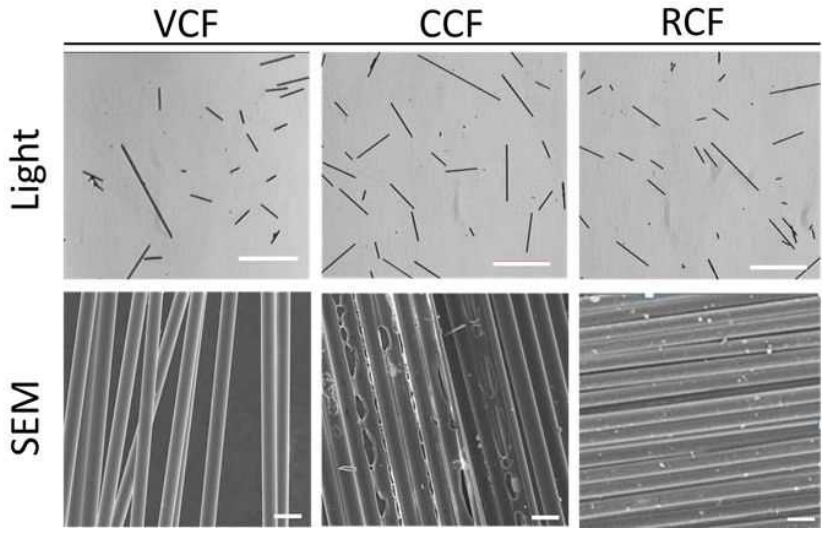

Fig. 13 Optical and Scanning Electron Microscope (SEM) images of carbon fibers

Optical and Scanning Electron Microscope (SEM) images for three types of carbon fibers. (Scale bars: light microscopy, 300 μm; SEM, 10 μm).

CFs were suspended in PBS solution. However, many carbon fibers have a length of 100 μm or more, and it has been difficult to disperse them as well as nanomaterials. Therefore, the suspended solution was stirred well before instillation.

Each carbon fiber suspension was intratracheally and intraperitoneally instilled once in mice. After instillation, the viability and general condition of the mice were observed once a week until dissection. The body weight of each mouse was measured once a week for 1 month, 6 months (intratracheal instillation), and 90 days (intraperitoneal instillation) post instillation. The average mouse body weight before the instillation treatment was approximately 25 g.

Statistically significant differences in the body weight loss of experimental animals were not observed between each carbon fiber group and the vehicle control

group at 1 month, 6 months (intratracheal instillation) and 90 days (intraperitoneal instillation) post-instillation (Fig. 14).

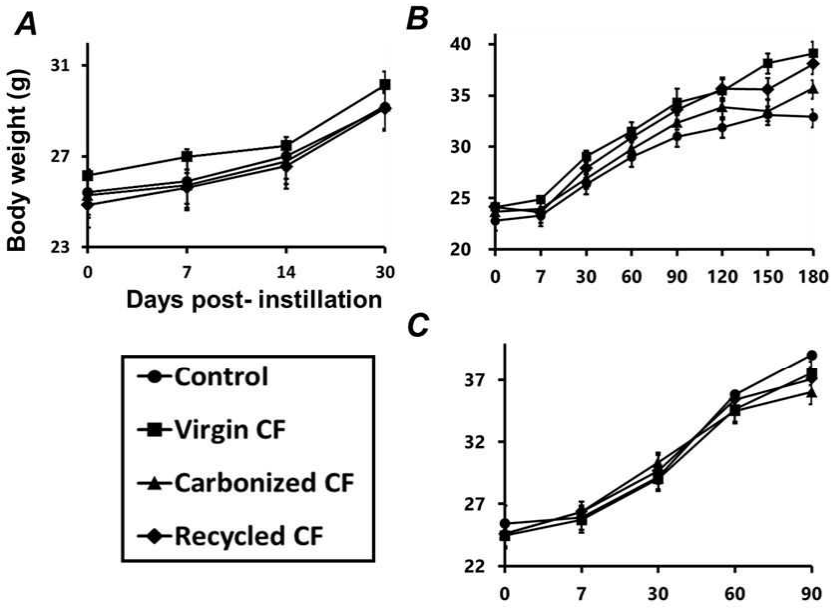

Fig. 14 Body weight of mice after instillation of carbon fibers

(A)Intratracheal instillation for 1month (B) Intratracheal instillation for 6months (C) Intraperitoneal instillation; the vehicle control (50 μL PBS per mouse; control) and the carbon fibers (0.2 mg Virgin, Carbonized, and Recycled carbon fibers per mouse) groups. Values are mean±S.E.

No clinical signs, such as abnormal behavior and irregular respiration, were observed during the observation period in any of the groups. Deaths during breeding were not observed in any of the groups except for the dissection performed at 1 month after intraperitoneal instillation to confirm abnormalities of the abdominal cavity.

2-3-3-2 Anatomical observation

To study the effects of each carbon fiber type in vivo, mice were killed 1 month or 6 months (Intratracheal instillation) and 90 days (Intraperitoneal instillation) after an injection with 0.2 mg of Virgin CF, Carbonized CF, or Recycled CF. Distinct macroscopic differences in anatomical observations were not observed among the three carbon fiber types.

Histopathological findings of lungs stained with hematoxylin and eosin showed that inflammatory cell infiltration was barely discerned in each of the experimental groups (Fig. 15). No clinical signs, such as phagocytosis by persistent alveolar macrophages, were observed in the alveoli, alveolar wall and bronchioles in any of the groups during the observation period. Carbon fiber was stuck in the tissue, but no abnormality could be confirmed around it (Fig. 15C).

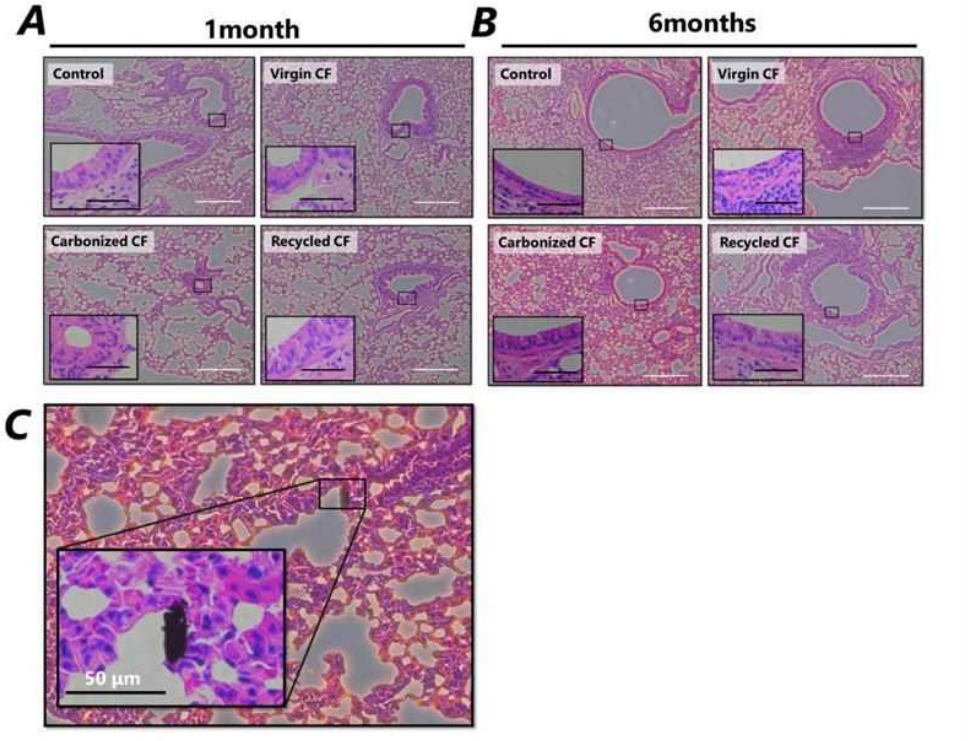

Fig. 15 Micrographs of lungs stained with hematoxylin and eosin
Image of lung tissue from a mouse exposed to CFs at 1month (A and C) and 6months (B) post-instillation. After the mice were sacrificed, the lung tissues were fixed in 4% buffered paraformaldehyde, followed by embedding in paraffin, and the sections were stained with hematoxylin and eosin. (black scale bars: 50μm, white scale bars: 200μm).

2-3-3-3 Gene expression analysis

Comprehensive analysis of gene expression profiles was performed using a DNA microarray. From the results, 85, 303, and 96 genes exhibited more than 2-fold higher intensities (treatment/control), and 65, 900, and 188 genes exhibited more than 0.5-fold lower intensities (treatment/control) under instillations of VCF, CCF, and RCF, respectively at 1 month post-instillation. The highest number of significantly altered genes was in CCF (2-fold; 303, 0.5-fold; 900). Meanwhile, 228, 183, and 40 genes exhibited more than 2-fold higher intensities (treatment/control) and 12, 9, and 12 genes exhibited more than 0.5-fold lower intensities (treatment/control) under instillations of VCF, CCF, and RCF, respectively at 6 months post-instillation (Table 14).

Table 14 The number of the up and down-regulated genes in each instillation condition

	1month			6months		
	VCF	CCF	RCF	VCF	CCF	RCF
Up-regulated	85	303	96	228	183	40
Down-regulated	65	900	188	12	9	12

The function of the induced gene at 1 month post-instillation was roughly similar in all CF groups. However, as in “immune system process” (GO: 0002376, VCF) or “signaling” (GO: 0023052, CCF), the inductive function unique to each CF was also confirmed (Table 15).

Table 15 Functional categories of the genes up-regulated at 1month post-instillation

GO ID	GO term	Number in the group	Number changed		
			VCF	CCF	RCF
GO:0008152	metabolic process	10880	35	145	47
GO:0051179	localization	5623	22	72	30
GO:0002376	immune system process	2342	17	0	0
GO:0032502	developmental process	5983	22	74	0
GO:0023052	signaling	6171	0	78	0

In the function of the induced gene at 6 months post-instillation, “detoxification” (GO: 0098754), “immune system process” (GO: 0002376) and “developmental process” (GO: 0032502) were common in all CF group (Table 16).

Table 16 Functional categories of the genes up-regulated at 6months post-instillation

GO ID	GO term	Number in the group	Number changed		
			VCF	CCF	RCF
GO:0002376	Immune system process	2342	25	31	10
GO:0032502	developmental process	5983	51	71	13
GO:0050896	response to stimulus	8942	72	80	17
GO:0098754	detoxification	29	3	3	3
GO:0022414	reproductive process	1670	0	24	0

Further, “response to stimulus” (GO: 0050896) contains “cellular response to DNA damage stimulus” (GO: 0006974) as a downstream term and the reproductive process is the term related to the genetics and the condition of the chromosome, so the expression of the genes related to DNA damage or cancer were compared with the other CF group (Fig. 16).

Genes involved in DNA damage and prognostic markers of lung cancer[44] are not induced at 1 month, but these were induced in the CCF group especially at 6 months post-instillation (Fig. 16A and B). However, the expression of markers predicting lung

tissue damage[45] is completely alleviated at 6 months post-instillation (Fig. 16B). These markers are gene induced when SWCNT is exposed for a long time and these are considered as potential biomarkers in lung tissue after SWCNT instillation[45]. These results suggested that this CF does not cause long-term tissue damage from the point of view of gene expression.

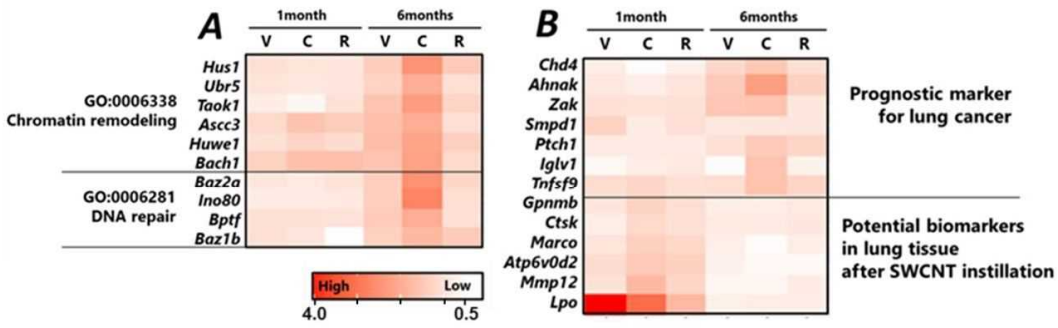

Fig. 16 Selected list of expressed genes related to DNA damage and bio-maker genes related to cancer or tissue damage. The color is based on values of gene expression fold change compared to vehicle control levels.(A) genes involved in the function category of “chromatin remodeling” and ”DNA repair” (B) bio-maker genes related to cancer or tissue damage.

In this study, three types of carbon fibers (CFs) were intratracheally or intraperitoneally instilled once. However, in all CF groups, the no aggravation effect was observed in the general condition and histopathological analysis. On the other hand, at the level of gene expression, differences were confirmed for each CF group. Especially, there was a significant difference in the suppression of genes. Generally, the suppression of gene expression indicates some stress in organisms. The suppression of gene expression suggested that the organism is trying to lower life activity. However, since the suppression of gene expression has been alleviated in all CF groups after 6 months, it is presumed that the stress was not acute or enormous and was at a level that could be removed in vivo (Table 14).

Regarding the function of induced genes, the expression of prognostic biomarker genes related to mutagenicity and lung cancer in the CCF group was confirmed.

The category of “hemoglobin complex” (GO: 0005833) contains the genes such as Hba-a1, Hba-a2 and Hbb-b1, and these genes are also involved in “detoxification” (GO:

0098754). Hemoglobin alpha, adult chain 1 (Hba-a1), hemoglobin alpha, adult chain 2 (Hba-a2) and hemoglobin, beta adult major chain (Hbb-b1) all consist of a tetramer hemoglobin molecule with γ or δ-globin chains, coordinate oxygen transport and bind with iron ions[46]. Hemoglobin and iron are known to be related to oxidative stress, and thus may be toxic to tissue[47, 48]. Therefore, we investigated the expression of other genes involved in oxidative stress (Table 17).

Table 17 Selected list of expressed genes involved in response to oxidative stress after intratracheal instillation with carbon fibers

Gene name	1month			6months			Description
	VCF	CCF	RCF	VCF	CCF	RCF	
Gpx1	0.91	0.85	0.98	0.89	0.92	0.91	Glutathione peroxidase1
Gpx3	1.13	1.07	0.58	0.95	0.99	0.89	Glutathione peroxidase3
Gss	0.76	0.79	0.84	0.97	1.01	1.49	Glutathione synthetase
Hmox1	0.87	1.04	0.91	0.72	0.78	0.68	Heme oxygenase1
Sod1	1.03	0.89	0.90	1.02	0.96	0.99	Superoxide dismutase1
Sod2	1.11	1.27	1.06	0.96	0.96	0.99	Superoxide dismutase2
Hba-a1	0.34	1.25	1.03	**3.37**	**2.35**	**2.71**	Hemoglobin alpha, adult chain 1
Hba-a2	0.52	0.87	0.88	**3.28**	**2.29**	**2.64**	Hemoglobin alpha, adult chain 2
Hbb-b1	0.38	1.66	0.69	**3.86**	**2.93**	**3.20**	Hemoglobin, beta adult major chain

The Hba-a1, Hba-a2, and Hbb-b1 genes exhibited a similarly high expression pattern at 6 months post-instillation in all CF groups, but the expression of other representative genes involved in the response to oxidative stress – such as the genes Gpx1, Gpx3, Gss, Hmox1, Sod1, and Sod2 – was scarcely altered in both time points. This suggests that these genes (Hba-a1, Hba-a2, and Hbb-b1) were not induced due to oxidative stress. Furthermore, the results of qPCR revealed that these detoxification genes are significantly induced at 6 months, though induction is small at 1 month (Fig. 17). Since this symptom is common to all CF groups, it is suggested as a gene induced when carbon fiber is latent in the body for a long time. This is expected to become a biomarker gene for long-term exposure of carbon fibrous material.

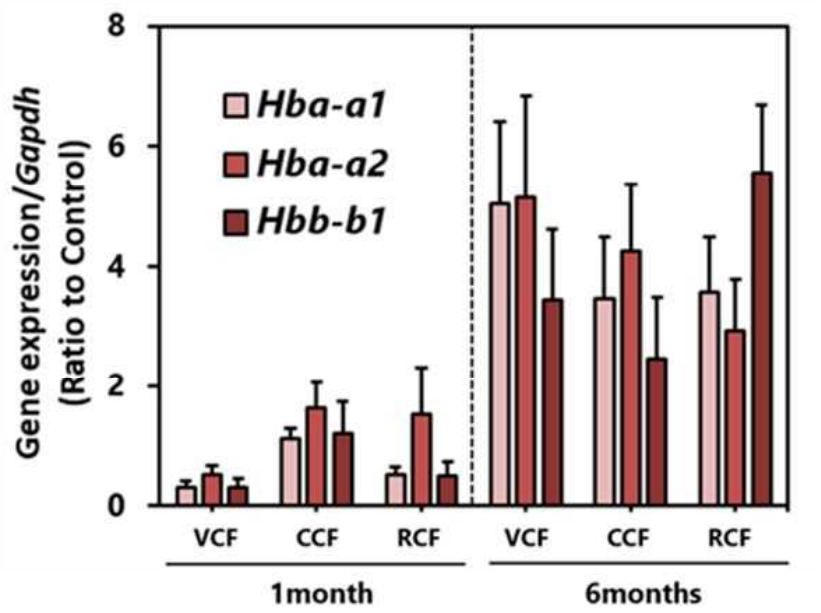

Fig. 17 Gene expression in the lung tissue of carbon fiber injected mice. VCF, CCF, RCF and PBS were administered to mouse lungs by intratracheal instillation. Gene expression was determined by real-time PCR. The values represent the mean ±SE.

Why would the differences occur among CF groups? We investigated the state of the fiber at the time of exposure, but no significant difference was confirmed between the number of fibers administered and the length of the fiber (Fig. 18).

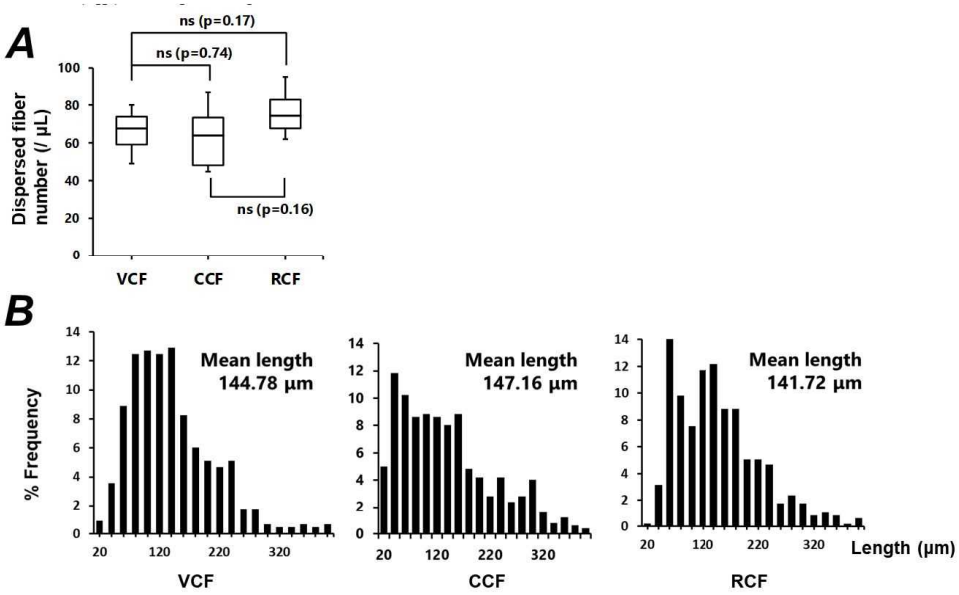

Fig. 18 Fiber Characteristics (A) Number of dispersed fibers in 4 mg/mL fiber suspensions. (B) Distribution of the lengths of each CF. To determine the number of dispersed fibers in suspension, 4 mg/mL of the fiber suspensions was diluted to 0.4 mg/mL in PBS. The diluted solution was then observed under a light microscope (BX-53, Olympus Corporation, Tokyo, Japan). The lengths and of each fiber were determined by measuring at least 500 fibers with a light microscope (BX-53).

This indicates that the influence on gene expression does not depend on the physical state of the fiber. Since the CCF group showed stress like carcinogenicity, it was suggested that impurities (such as dioxins) attached to the fiber may impart toxicity in vivo. Moreover, it is considered that RCF does not receive conspicuous stress after the long-term test by decomposition of impurities through the firing process. From these results, it is considered that this CFRP recycling is very useful, not only from the viewpoint of energy, but also from that of safety.

In recent years, not only carbon nanotube or carbon fiber, the development of carbon-based nanomaterials such as graphene[49] has increased and is expected to expand into diverse industrial fields. In this study, we evaluated the harmfulness of carbon fiber generated in the new recycling process. We believe that an assessment of harmfulness and biological effect of new materials should be considered.

3. CONCLUSION

We assessed the effects of TiO_2-NOAAs on yeast under UV irradiation. The result of the DNA microarray analysis, suggested that yeast cells that are adsorbed by TiO_2-NOAA under UV irradiation suffer oxidative stress. However, the quantitative PCR results suggested that the oxidative stress is caused not by the TiO_2 nanoparticles but by UV. It also suggested that TiO_2-NOAAs without UV irradiation damage the membranes of yeast cells, which induces yeast cells to synthesize glycogen and trehalose. Thus, we concluded that the role of TiO_2-NOAAs on yeast under UV irradiation is protection of UV irradiation like sun cream, not to cause stress.

Next, we carried out a catch ball analysis of yttrium oxide and yttrium ion toxicities and the results indicate that yeast cells undergo oxidative stress after Y_2O_3 nanoparticle (20 mg/5 ml) and YCl_3 (5 mg/5 ml) treatment. We conclude that Y_2O_3 nanoparticle toxicity is due to oxidative stress and protein denaturation caused by the yttrium ions derived from the Y_2O_3 nanoparticles and the nanoparticles themselves were not the cause of the toxicity. The toxicity can be caused by the minor part of solubilized Y^{3+} ions while the measure parts of dissolved ions were precipitation with medium component. Those solubilized Y^{3+} ions induce oxidative stress and cause protein denaturation, thereby stimulating proteasome formation to eliminate denatured proteins. The results show that yttrium nanoparticles induce oxidative stress that has often associated with heavy metal ions. Thus, the use of yttrium nanoparticles or yttrium ion must be controlled like heavy metals.

Several investigators have demonstrated that industrial materials such as CNTs can elicit toxicity, including the initiation of an acute, neutrophil-driven inflammatory response, oxidative stress, granuloma formation, and fibrosis. Therefore, broad conclusions may be postulated regarding the mechanisms underlying fibrous material toxicity[42, 48 50, 51]. In this study, we illustrated an approach for investigating recycled carbon fiber toxicity using gene expression, together with histopathological findings.

In this study, we showed that CF groups do not exhibit acute toxicity like CNT or asbestos. Furthermore, from the results of gene expression, carbon fiber under recycling (CCF) was found to have toxicity like mutagenicity, which appears after long-term observation. This symptom was not confirmed in mice injected with recycled carbon fiber (RCF). These results showed that not only the safety of this recycling process, but also the toxicity of the fibrous material is due to the inherent impurities rather than the

physical factors.

As described above, the toxicity of industrial materials may be affected by secondary factors such as increased solubility, cohesion, and adsorptivity. Moreover, evaluation is necessary because surface treatment agents and impurities may have a biological effect. Accurate safety assessment leads to the elucidation of toxicity mechanisms and the development of safer industrial materials.

4. ACKNOWLEDGEMENT

I would like to thank Dr. Hitoshi Iwahashi of Gifu University for giving me an opportunity to study in his laboratory. I must thank for his valuable suggestions and guidance.

I'm also thankful to Dr. Tomoyuki Nakagawa, Dr. Masanori Horie, Dr. Tomonori Iwama, Dr. Hiroshi Moritomi and Dr. Junko Takahashi for sharing their technical and scientific knowledge without any reservation to conduct this research.

I also express thank to Mr. Takema Hasegawa and other students in Applied Microbiology Laboratory of Gifu University for their earnest help.

5. REFERENCE

1 ISO/TS 80004-2:2015 Nanotechnologies --Vocabulary-- Part 2: Nano-objects

2 M Horie, H. Kato, K. Fujita, S. Endoh, and H. Iwahashi, *Chemical Research in Toxicology.* 25, 3 **(2012).**

3 EPA, External Review Draft, Nanomaterial Case Studies: Nanoscale Titanium Dioxide in Water Treatment and in Topical Sunscreen. United States Environmental Protection Agency **(2009)**.

4 M. Andrew, and LH. Stephen, *Journal of Photochemistry and Photobiology A: Chemistry* 108, 1**(1997)**.

5 AF. Howard, BD. Iram, V. Sajnu, and S. Alex, *Applied Microbiology and Biotechnology* 90 **(2011)**.

6 ISO/TR 13014, Nanotechnologies - Guidance on physico-chemical characterization of engineered nanoscale materials for toxicologic assessment **(2012).**

7 I. Yamada, K. Nomura, H. Iwahashi, and M. Horie, *Chemosphere* 143 **(2016)**.

8 Y. Momose, H. Iwahashi, *Environmental Toxicology and Chemistry* 20,10 **(2001)**.

9 H. Iwahashi, K. Obuchi, S. Fujii, and Y. Komatsu, *Cellular and molecular biology* 41, 6 **(1995)**.

10 UA. Akalpita, and BP. Narayan, *Yeast,* 19 **(2002)**.

11 AP. Gasch, Yeast Stress Responses *Topics in Current Genetics* 1 **(2002)**.

12 LH. Eduardo, LC. Wayne, J. Barbara, AG. Ian, and B. Alison, *The EMBO Journal* 19, 24 **(2000)**.

13 ISO Standards Website;http://www.iso.org/iso/home/store/catalogue_tc/catalogue_detail.htm?csnumber=54440.

14 M. Horie, K. Fujita, H. Kato, S. Endoh, K. Nishio, L. Komaba, A. Nakamura, A. Miyauchi, S. Kinugasa, Y. Hagihara, E. Niki, Y. Yoshida, and H. Iwahashi, *Metallomics* 4, 350 **(2012)**.

15. I. Pujalté, I. Passagne, B. Brouillaud, M. Tréguer, E. Durand, C. Ohayon-Courtès, and B. L'Azou, *Part Fibre. Toxicol.* 3, 8 **(2011)**.

16. HL. Karlsson, P. Cronholm, J. Gustafsson, and L. Möller, *Chem. Res. Toxicol*. 9, 26 **(2008)**.

17 M. Horie, K. Nishio, K. Fujita, H. Kato, A. Nakamura, S. Kinugasa, S. Endoh, A. Miyauchi, K. Yamamoto, H. Murayama, E. Niki, H. Iwahashi, Y. Yoshida, and J. Nakanishi, *Chem. Res. Toxicol.* 22, 1415 **(2009)**.

18 B. Fahmy and SA. Cormier, *Toxicol. In Vitro* 23, 1365 **(2009)**.

19 R. Roy, A. Tripathi, M. Das, and PD. Dwivedi, J. Biomed. *Nanotechnol*.7, 110 **(2011)**.
20 ISO Standards Website; http://www.iso.org/iso/home/store/catalogue_tc/catalogue_tc_browse.htm?commid=381983.
21 T. Andelman, S. Gordonov, G. Busto, PV. Moghe, and RE. Riman, *Nanoscale Research Letters* 5, 263 **(2009)**.
22 V. Selvaraj, S. Bodapati, E. Murray, KM. Rice, N. Winston, T. Shokuhfar, Y. Zhao, and E. Blough, *International Journal of Nanomedicine*. 9, 1379 **(2014)**.
23 A. Hosseini, AM. Sharifi, M. Abdollahi, R. Najafi, M. Baeeri, S. Rayegan, J. Cheshmehnour, S. Hassani, Z. Bayrami, and M. Safa, *Biol. Trace Elem. Res*. 164, 80 **(2015)**.
24 D. Yasokawa and H. Iwahashi, *J. Biosci. Bioeng*. 110, 511 **(2010)**.
25 G. Liti, DM. Carter, AM. Moses, J. Warringer, L. Parts, SA. James, RP. Davey, IN. Roberts, A. Burt, V. Koufopanou, IJ. Tsai, CM. Bergman, D. Bensasson, MJT. O'Kelly, AV. Oudenaarden, DBH. Barton, E. Bailes, AN. Nguyen, M. Jones, MA. Quail, I. Goodhead, S. Sims, F. Smith, A. Blomberg, R. Durbin, and EJ. Louis, *Nature* 458, 337 **(2009)**.
26 CC. Barbacioru, Y. Wang, RD. Canales, YA. Sun, DN. Keys, F. Chan, KA. Poulter, and RR. Samaha, *BMC Bioinformatics* 7, 533 **(2006)**.
27 X. Lin, J. Li, S. Ma, G. Liu, K. Yang, M. Tong, and D. Lin, PLoS One 9, 1 (2014).
28 N. Zhang, J. Hou, S. Chen, C. Xiong, H. Liu, Y. Jin, J. Wang, Q. He, R. Zhao, and Z. Nie, *Scientific Reports* 6, 1 **(2016)**.
29 J. He, X. Zhu, Z. Qi, C. Wang, X. Mao, C. Zhu, Z. He, M. Li, and Z. Tang, *ACS Appl. Mater. Interfaces* 7, 5605 **(2015)**.
30 M. Rep, M. Proft, F. Remize, M. Tamás, R. Serrano, JM. Thevelein, and S. Hohmann, *Mol. Microbiol.* 40, 1067 **(2001)**.
31 MI. González-Siso, A. García-Leiro, N. Tarrío, and ME. Cerdán, Microb. *Cell Fact* 30, 8 **(2009)**.
32 VK. Singh and J. Moskovitz, *Microbiology* 149, 2739 **(2003)**.
33 S. Boschi-Muller, A. Gand, and G. Branlant, *Arch. Biochem. Biophys.* 474, 266 **(2008)**.
34 M. Schrader and HD. Fahimi, *Biochim. Biophys. Acta*. 12, 1755 **(2006)**.
35 MJ. Tamás, SK. Sharma, S. Ibstedt, T. Jacobson, and P. Christen, *Biomolecules* 4, 252 **(2014)**.
36 D. Yasokawa, S. Murata, E. Kitagawa, Y. Iwahashi, R. Nakagawa, T. Hashido, and

H. Iwahashi, *Environmental Toxicology* 23, 599 **(2008)**.
37 D. Cavallo, C. Fanizza, CL. Ursini, S. Casciardi, E. Paba, A. Ciervo, et al. *J Appl Toxicol*. 32 **(2012)**.
38 H. Haniu, N. Saito, Y. Matsuda, T. Tsukahara, K. Maruyama, Y. Usui, et al. *Toxicol In Vitro*. 27 **(2013)**.
39 S. Hirano, Y. Fujitani, A. Furuyama, and S. Kanno. *Toxicol Appl Pharmacol* 249 **(2010)**.
40 CA. Poland, R. Duffin, I. Kinloch, A. Maynard, WA. Wallace, A. Seaton, et al. *Nat Nanotechnol* 3 **(2008)**.
41 K. Donaldson, FA. Murphy, R. Duffin, CA. Poland.. *Part Fibre Toxicol*. 7,5 **(2010)**.
42 H. Nagai, Y. Okazaki, SH. Chew, et al. *Proc Natl Acad Sci USA* 108, 49 **(2011)**.
43 KJ. Livak, TD. Schmittgen. *Methods.* 25 **(2001)**.
44 M. Pacurari, Y. Qian, DW. Porter, M. Wolfarth, Y. Wan, D. Luo, M. Ding, V. Castranova, and NL. Guo. *Toxicol Appl Pharmacol*.255, 1 **(2011)**.
45 K. Fujita, M. Fukuda, H. Fukui, et al. *Nanotoxicology* 9, 3 **(2014)**.
46 H. Dassen, R. Kamps, C. Punyadeera, F. Dijcks, et al. *Hum Reprod* 23, 3 **(2008)**.
47 NG. Abraham, Y. Lavrovsky, ML. Schwartzman, RA. Stoltz, RD. Levere, ME. Gerritsen, S. Shibahara, A. Kappas. *Proc Natl Acad Sci U S A* 92, 15 **(1995)**.
48 J. Balla, HS. Jacob, G. Balla, K. Nath, JW. Eaton, GM. Vercellotti. Endothelial-cell heme uptake from heme proteins: induction of sensitization and desensitization to oxidant damage. *Proc Natl Acad Sci U S A* 90, 20 **(1993)**.
49 P. Jinbo, GM. Rafael, SW. Pawel, DW. Michal, QT. Huy, Z. Liang, G. Lars, T. Barbara, G. Thomas, F. Lei, L. Zhongfan, E. Juergen, B. Alicja, HR. Mark. *ACS Nano* 11, 2 **(2017)**.
50 J. Dong, Q. Ma. *Nanotoxicology* 9, 5 **(2015)**.
51 HJ. Johnston, GR. Hutchison, FM. Christensen, et al, *Nanotoxicology* 4, 2 **(2010)**.